TECHNISCHE
UNIVERSITÄT
WIEN
Vienna University of Technology

MASTERTHESIS

Hydrogenation and Transfer Hydrogenation of Aromatic Ketones using Iron(II) Pincer Complexes

performed at

Institute for Applied Synthetic Chemistry (UT Vienna)

Research Group Organometallic Chemistry

under Supervision of

a.o. Prof. Dr. Karl Kirchner,

Prof. Dr. Kazushi Mashima

and Dr. Christina Standfest-Hauser

by

Gerald Bauer

Matr.-Nr. 0426337

A-3441 Pixendorf; Quellenweg 1

Vienna, November 2010

‚Erfolg in der Forschung benötigt 4 G's:
Glück, Geduld, Geschick und Geld!'

Paul Ehrlich
Father of Chemotherapy

1 Abstract

The aim of this work was to utilize Fe(II) PNP-pincer complexes for the reduction of aromatic ketones. The compounds used for this task were previously developed by our group and already successfully applied in the field of chemoselective cross coupling of diazoacetates with aromatic aldehydes.

In the first part this work the reaction conditions for the hydrogenation reactions were optimzed and different complexes were screened for their catalytical activity towards aromatic ketones. We were able to show that *trans*-[Fe(PNP-*i*Pr)(CO)Cl_2] converts 99.4% of acetophenone in a 0.2 mol L^{-1} solution at 50ºC and 30bar H_2 pressure. In addition we discovered interesting details concerning the mechanism of the iron catalyzed hydrogenation which, in the future, may be helpful for the elucidation of a detailed overall mechanism.

In the second part of this thesis the catalytic activity of Fe(II) PNP-pincer complexes in the hydrogen transfer from *iso*-propanol to acetophenone was investigated. We were able to show that these complexes albeit in poor yields are capable of performing transfer hydrogenation. In order to make the yields competitive to already commercially used precious metal catalysts, the base concentration had to be raised. Unfortunately a higher base concentration resulted in more side reactions. Accordingly, the big advantages of iron catalyzed transfer hydrogenation are rather limited for this particular system, i.e., Fe(II) PNP-pincer complexes based on aminophosphines.

2 Zusammenfassung

Die Aufgabe dieser Arbeit war es Eisen (II) PNP-Pincer Komplexe zur Reduktion von aromatischen Ketonen anzuwenden. Die für diese Aufgabe benötigten Komplexe wurden im Vorfeld von unserer Gruppe entwickelt und bereits zur Kupplung von Diazoazetaten mit aromatischen Aldehyden eingesetzt.

Im ersten Teil wurden zuerst die idealen Reaktionsbedingungen erarbeitet und in weiterer Folge die Komplexe auf ihre katalytische Aktivität hinsichtlich aromatischer Ketone geprüft. Es konnte gezeigt werden, dass *trans*-[Fe(PNP-*i*Pr)(CO)Cl_2] 99,4% Acetophenon in einer 0,2 molaren Lösung bei milden Bedingungen – von 50ºC und 30 bar H_2 Druck – umsetzt. Zusätzlich wurden fundamentale Erkenntnisse über einen möglichen Reaktionsmechanismus gefunden, die es bei weiterer Forschung ermöglichen, einen vollständigen Mechanismus zu beschreiben.

Im zweiten Teil wurde nach der katalytischen Aktivität selbiger Komplexe hinsichtlich des Transfers von Wasserstoff von *iso*-Propanol zu Acetophenon geprüft. Es konnte gezeigt werden, dass die Komplexe fähig sind Transferhydrierung durchzuführen. Die Umsätze sind aber zu gering, um mit kommerziell verwendeten Edelmetallkatalysatoren in Konkurrenz zu treten. Um sie wettbewerbsfähig zu machen, müsste die Basenkonzentration angehoben werden, was aber wiederum zu einer Erhöhung der Nebenreaktionen führen würde, die durch die Basen katalysiert werden. Alles in Allem beschränken die begrenzenden Reaktionsbedingungen die vielfältige Einsetzbarkeit der Transferhydrierung, welche in weiterer Folge auch die Einsetzbarkeit von Fe(II) PNP-Pincer Komplexe in diesem Feld beschränken.

3 Acknowledgements

I really want to thank everyone who supported me, and helped me finishing my diploma thesis. It would be too much to name everyone, and it would be awkward, if I miss someone, but in fact, there are some people whom I really want to thank for:

First of all there are my parents and my family who gave me all the financial and moral support to proceed in my studies. Without them I would not be at the point I am today.

I also want to thank my supervisor, Karl Kirchner, who offered me a really interesting and promising topic, and his guidance through the whole thesis. It was a pleasure to get a good and widespread insight into organometallic chemistry.

In addition I want to thank my lab mates Christina, Maria, Bernhard, Christian, and Özgür for the good working atmosphere, and their time during the coffee and lunch brakes.

I want to thank Kazushi Mashima for inviting me over to Osaka, and the UT Vienna and the GCOE Progamm for financing this trip. They gave me a total novel point of view. It was really a fruitful and live changing experience to see and live Japanese culture.

In addition I want to thank Mashima's lab in particular Takuto, Das-san, Shin, Shinji, Kawata-san, Hiroshi, Hiro, and all the others for introducing me into Japanese culture and life, especially Takuto who always was a huge support. He will stay in my mind as the raw model of a hard working Japanese chemist.

Finally I thank my friends Brigitte and Philipp who were always around in University, for learning, coffee breaks, and also in the free time. They really were supportive and without them it would have been a hard time to finish my studies.

4 Table of Content

5 List of Figures

6 List of Schemes

7 List of Tables

8 Introduction and Scope

Catalytic hydrogenations and transfer hydrogenations of various functional groups – *e.g.* C=C, C=O – are among the most important reactions in modern organic synthesis. Of particular importance are carbonyl compounds, since they are easily accessible through a huge pallet of different reactions like condensation reactions forming mainly β-carbonyl compounds, and Friedel-Craft acylation forming aryl-alkyl ketones. Due to their – sometimes – prochiral character a vast majority of enantiomerically pure compounds is accessible through asymmetric catalytic reduction methods.

Historically there is a large amount of different well-established reduction reactions. However, there is still a big potential for organometallic chemists to develop new catalytic systems with even higher activities and efficiencies. The most common transition metals used in this field are precious platinum group metals like ruthenium, rhodium, platinum, and palladium. Catalysts containing these elements have been investigated for a long time and are already well-proven as highly active and selective catalysts. Due to their high price and their toxicity they are sometimes problematic for industrial scale use. Therefore the demand for more ecologic and economic alternatives is desirable. Alternatives were found in the utilization of first row transition metals like iron, copper, manganese, and zinc. Mainly in the last decade a hype in making chemistry more sustainable and “greener” broke out due to the scarcity of the resources and the demand of the industry to produce less (toxic) waste. Since then every year more and more remarkable results were found which might substitute precious metals in the near future.

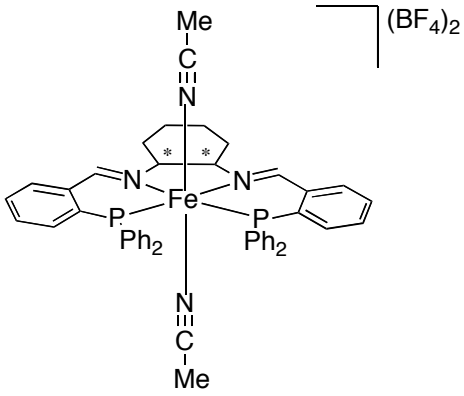

Figure 1: *trans*-[Fe(Ph-P_2N_2)AN_2]$(BF_4)_2$ developed by Morris and coworkers.

Surprisingly, there are only a few examples in the literature which successfully describe the use of iron complexes in the field of transfer hydrogenation and hydrogenation. Beller and coworkers used $Fe_3(CO)_{12}$ as pre-catalysts in combination with a porphyrine molecules to successfully transfer hydrogen from *iso*-propanol to carbonyls with very good results [1,2]. Furthermore, Morris and Gao developed Fe(II) P_2N_2 and $P_2(NH)_2$ complexes (Figure 1), which showed remarkable results in both hydrogenation and transfer hydrogenation [3-7]. Finally, Chirik and coworkers were able to use Fe(II) PNP-pincer complexes for the efficient hydrogenation of double bonds [8]. The ligands used in these systems feature imine, amine, and phosphine functionalities, which are all very strong donor ligands, a feature which is apparently crucial for hydrogenation and transfer hydrogenation reactions with respect to iron complexes.

Figure 2: General structure of a pincer complex.

For the last couple of years our group is dealing with the development of modular built bi- and tridentate ligand systems based on aminophosphines and the synthesis of transition metal complexes thereof (Figure 2). Since they feature

similar functional groups as the examples mentioned in the previous paragraph, it is reasonable to assume that they also exhibit catalytic activity for the reduction of carbonyls via hydrogenation and/or transfer hydrogenation. In a matter of fact this work can be considered as spearhead since exactly this type of complexes were only used for reducing double bonds but not carbonyls.

The objective of this work was to screen an already existing pallet of Fe(II) PNP-pincer complexes for their catalytic activity towards reduction of acetophenone and substituted acetophenone derivatives. The second target was to prepare and to characterized novel Fe(II) complexes which may be active and potential catalytic species for hydrogenation and/or transfer hydrogenation.

9 Ligands

9.1 Overview

The first catalytic methods for the reduction carbonyl compounds were using heterogeneous catalysts. Those catalysts were mainly based on 2nd and 3rd row platinum metal oxides [9], but also non-precious metal catalysts like Raney nickel [10]. They showed reasonable yields, but the reaction conditions were sometimes rather harsh, both in terms of temperature and H_2 pressure. In the mid 1960's Sir G. Wilkinson and coworkers performed pioneering work in homogeneous catalysis. They were coordinating the mono-dentate ligands Ph_3P, Ph_3As and Ph_3Sb to $RuCl_2$, $RuCl_3$ and $RhCl_3$ (Figure 3) and investigated their activity in the catalytic hydrogenation of olefins [11,12]. Right after Wilkinson L. Vaska synthesized a well-defined $Ir(CO)(PPh_3)_3$ complex which they used for the hydrogenation of ethylenes and acetylenes [13].

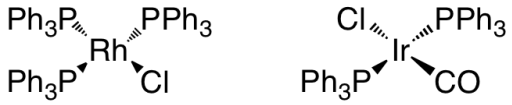

Figure 3: Examples for Wilkinson's - and Vaska's catalyst.

Decisive for the development of the ligands was the need of enantiomerically pure products. Until the 1960's enantiomerically pure compounds were only produced by biochemical methods or by producing a racemic mixture with further separation, a process usually more work intensive and costly than the synthesis itself [14]. Early methods of asymmetric hydrogenation date back to the mid 1950's when S. Akabori started to modify the heterogeneous palladium and Raney nickel catalyst with chiral reagents [15-18]. But the *ee*'s (enantiomeric excess) were still too low to compete with the conventional methods. Furthermore Mislow and Horner independently synthesized chiral phosphin compounds [19,20] and proved that they are stable towards inversion at room temperature and have a half-life at 115ºC of

several hours, albeit their nitrogen analogs rapidly change there chirality at room temperature [14]. The seminal work done by this groups led Knowles in 1968 to the idea of coordinating a chiral phosphine ligand to a metal center similar to Wilkinson's catalyst. The first experiment was the hydrogenation of α-phenylacrylic acid with a methylpropylphenylphosphin ligand, and it resulted in an *ee* of 15% (Scheme 1) [21]. Even though the *ee* was low they were on the right track with this approach.

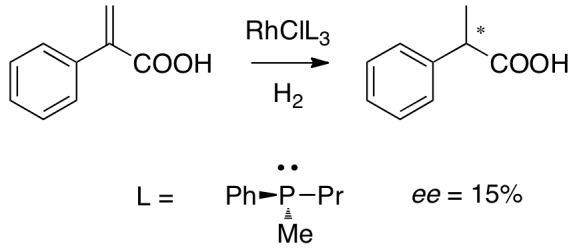

Scheme 1: Hydrogenation of α-phenyloacrylic acid with a Wilkinson type catalyst with a chiral ligand.

Thereafter an optimization of the catalytic system was carried out, mainly focusing on optimization of the phosphine ligand. Knowles believed that the hydrogen, the substrate and the phosphine ligand carrying the chiral information, have to be attached to the metal center at the same time [14]. Parallel to this work Morrison worked on phosphine ligands, where the chiral information was shifted from the phosphine to the carbon backbone of the ligand. They showed *ee*'s up to 61% using the prochiral (E)-2-methylcinamic acid with neomenthyldiphenylphosphine (NMDPP) as ligand (Scheme 2) [22]. These achievements opened the door to chiral bi- and polydentate ligands. Since then the phosphine ligands were refined and the *ee*'s were improving to > 99% [23].

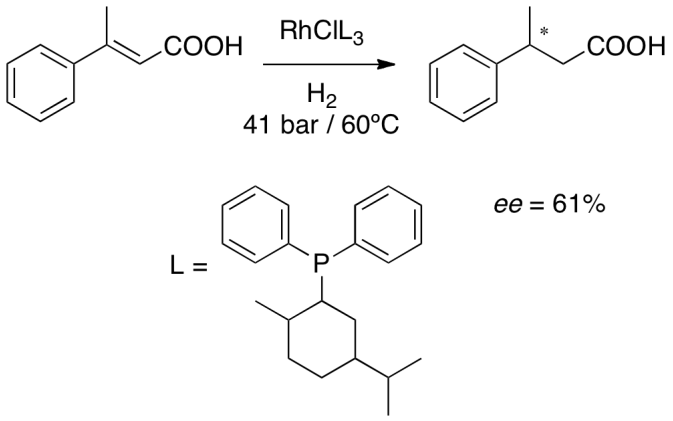

Scheme 2: Hydrogenation of β-methylcinnamic acid with NMDP as ligand.

9.2 Economic Issues

In order to design a ligand for industrial scale it is very important to keep the synthesis as simple as possible, since it is almost impossible to buy ready made ligands at a chemical supplier. Beside the costs for the metal precursors used for the catalysis, the ligands have an unusual and sometimes complicated structure, which are mostly made by multistep synthesis. As mentioned in the previous chapter, most of the ligands are based on phosphines, which make them strongly air sensitive and susceptible to oxygen. The total costs for a chiral diphosphine ligand are estimated to 100 – 500 $/g for laboratory scale batches and 5,000 – 20,000 $/kg for large-scale batches. Nitrogen and oxygen ligands which are often used for early transition metal complexes are usually cheaper [24].

9.3 Pincer Ligands

Pincer complexes are built up by coordinating a pincer ligand to a metal center (Figure 4). It is apparent that the planar chelating ligand binds to three coplanar sites. This form of complex was eponymous to this complex, since it looks like a pair of tweezers holding the metal center in the middle. This constrained structure also avoids cyclometalation by the donor sides and is also responsible for its high thermal stability.

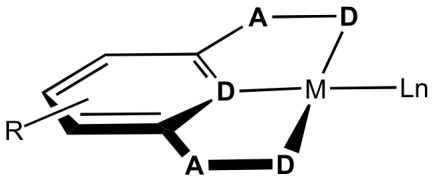

Figure 4: General structure of a pincer complex.

The aim of organometallic chemistry in the recent years is to develop well-designed ligand systems, which can be easily varied, and which themselves vary the properties of the metal center in a controlled manner [25]. The first pincer type ligands were described in the 1970's [26], but there has not been a lot of noticeable interest in this type of ligand. Starting in the 1990's pincer complexes attracted increasing interest (Figure 5) due to its well-defined geometrical properties, described in the previous paragraph.

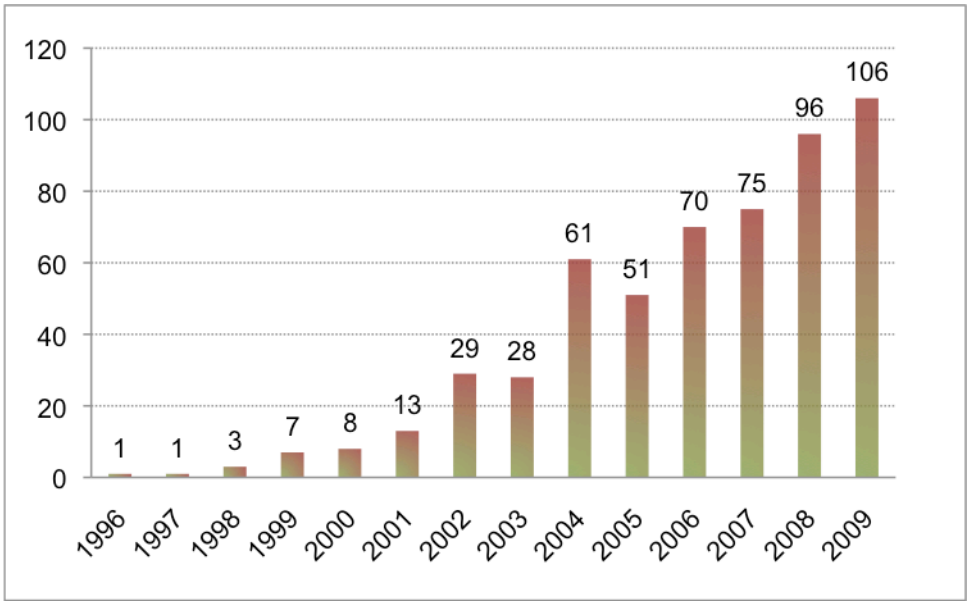

Figure 5: Number ob publications containing the word "Pincer Complex" [SciFinder].

The scaffold of this ligand (Figure 6) usually consists of an aromatic ring, which is either a (un)substituted benzene– (**D**C**D**) or a (un)substituted pyridine derivative (**D**N**D**). The aromatic system is connected to two electron-donating substituents (**D**), which are located in an *ortho*,*ortho*-position to the aromatic ring. This groups mainly consist of phosphine (–PR_2), phosphite (–$P(OR)_2$), also imine (=NR) and

amine (–NR_2) substituents and further ethers (–OR), thioethers (–SR), N-heterocyclic carbenes (NHC's), arsines (–AsR_2) and selenoethers (–SeR). The two side chains are connected with a spacer (**A**) to the aromatic ring. These spacers are usually methylene (–CH_2–), a single oxygen atom (–O–), or amine (–NR–) groups [25].

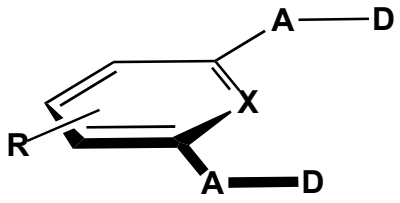

D = PR_3, $P(OR)_2$, NR_n, further OR, SR, AsR_2, SeR

A = CH_2, O, NR

X = C, N

R = Alkyl, Aryl, Acyl, ...

Figure 6: General model of a pincer ligand.

The two neutral donor substituents need not be identical [27]. Thus a large variety of different ligands is accessible only by varying **D**, **A**, **X**, and **R** (Figure 6). The largest group of pincer ligands are those, which are containing phosphorus in any oxidation state, as donating substituents, due to its good donor and acceptor properties [28]. Since there is no general method to prepare PNP and PCP pincer ligands using similar precursors, and also for the difficulty to introduce chirality into the ligand, our group found out that the use of an amine as a spacer between the aromatic ring and the phosphorus donor substituent allows formation of the link between P and N by a basic condensation reaction, using a phosphine- or phosphite chloride. This new synthetic strategy opens up a whole new modular synthetic strategy for a large field of different PNP and PCP ligands, where chirality can be easily introduced by using electrophilic chlorophosphines or –phosphites carrying the chiral information in the carbon backbone of the substituent (see Morrison *et. al.*, *vide* 9.1 Overview). Those compounds can usually be derived from the "chiral pool".

In the literature there are many ways to synthesize PNP and PCP pincer ligands, those synthetic pathways are depending on the spacer between the aromatic ring and the phosphine / phosphite substituent. A typical way to link the phosphorus derivative to a methylene spacer is the treatment of either 2,6-

bis(bromomethyl)pyridine or 1,3-bis(bromomethyl)benzene with *in situ* prepared lithium phosphides. PCP Pincer ligands bearing oxygen spacers, who are also called phosphinito pincer complexes, are typically prepared from resorcinol with chlorophosphines, analogous to Pincer ligands with an amine-spacer. More difficult is the synthesis of phosphinito PNP ligands, hence the 2,6-dihydroxypyridine tautomerizes to 6-hydroxypyridine-2-one, which makes the condensation with both hydroxy groups very difficult, or almost impossible. As briefly mentioned in the previous paragraph, the third method is the use of amine spacers. This synthesis is straightforward and performed by condensing a chlorophosphine with a primary or secondary amine in the presence of an amine base. With this set of synthetic instruments it is possible to synthesize a large set of different PNP and PCP ligands (Scheme 3). The synthesis of the different chlorophosphites – chiral and achiral – is achieved by simply reacting diols and amino-alcohols with phosphorus trichloride [25].

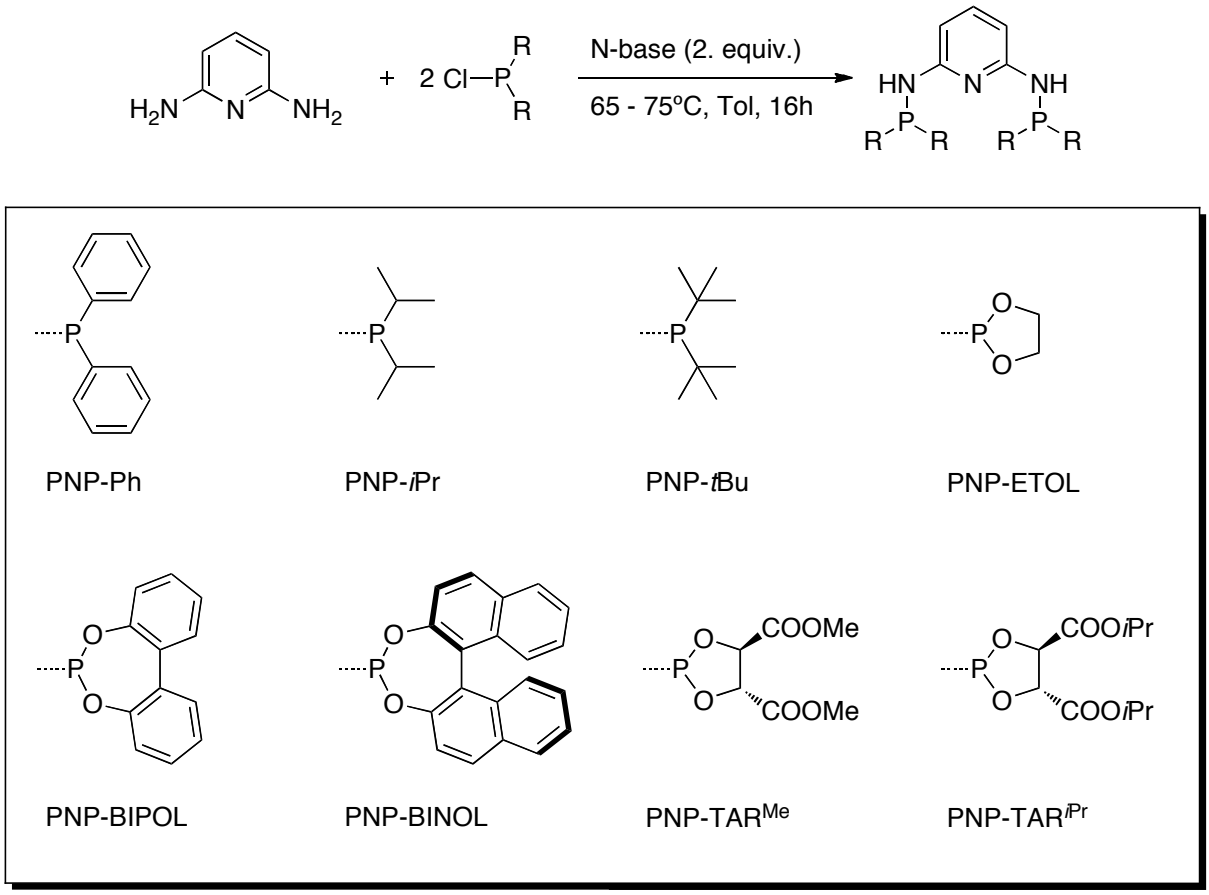

Scheme 3: Palette of PNP ligands synthesized by our group [25].

9.4 Pincer Complexes

The synthesis of the metal complexes is performed in a straightforward manner, by mixing the ligand with an appropriate metal precursor in polar solvents, like acetone, acetonitrile, THF or similar. The solution immediately changes color, and the complex solution can be worked up after about 1-2 hours by evaporating the solvent until a concentrated solution remains. The complex is precipitated by slowly adding Et_2O (diethylether). The solid is isolated by filtration and washed with Et_2O twice.

The choice of the metal precursor and solvent strongly depends on the resulting complex (Scheme 4). Our group recently carried out a big screening on molybdenum, nickel, platinum, palladium, ruthenium, and iron PNP complexes.

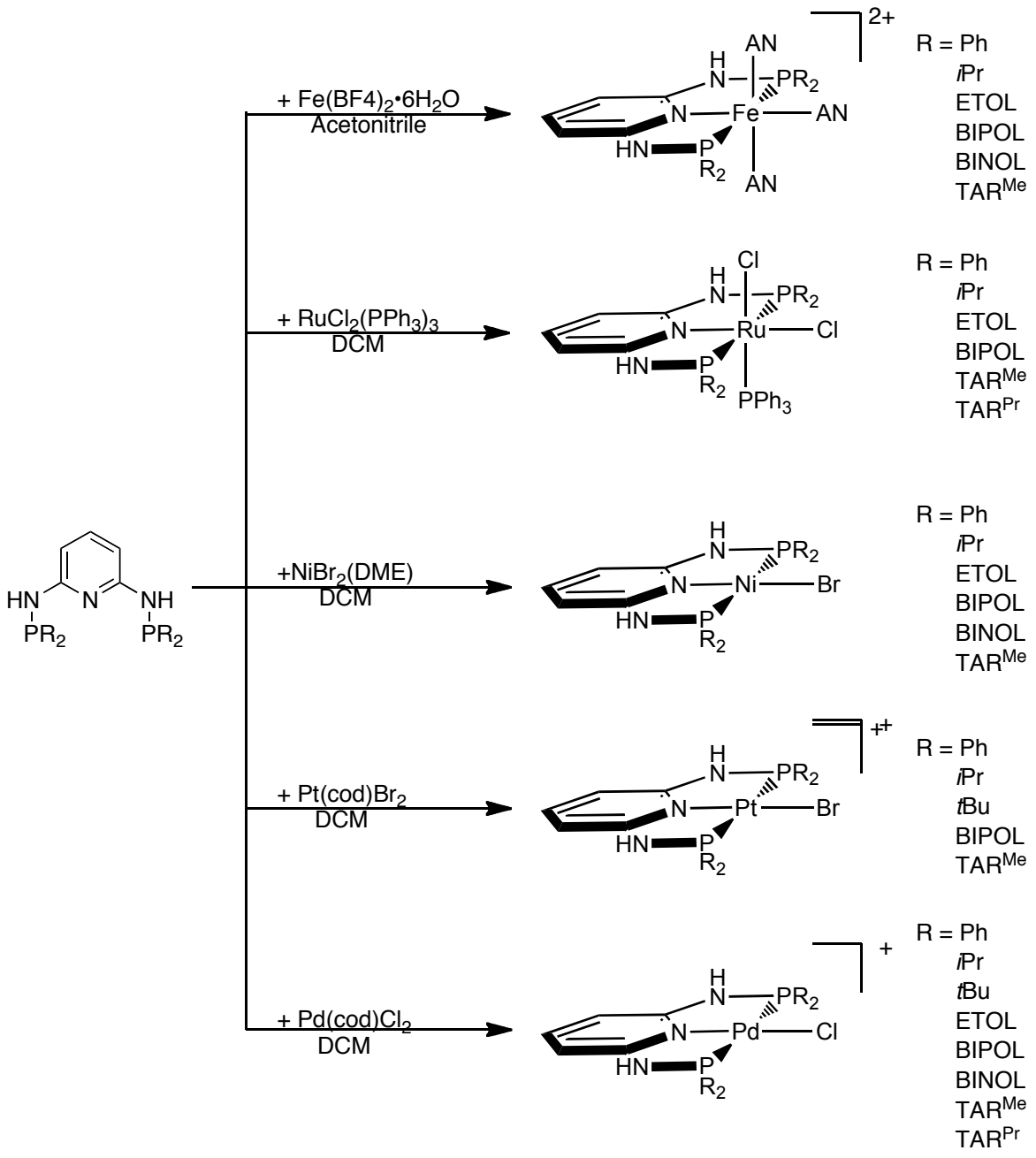

Scheme 4: Reaction scheme for complexing various PNP-pincer complexes [25].

9.5 Applications

Due to their high thermal stability, variability, and flexibility pincer complexes are gaining more and more interest in the field of homogenous catalysis. Catalytic applications of pincer complexes have been reported in the field of asymmetric aldol condensation of methyl isocyanoacetate, and aldehydes, carbonyl reduction

by hydrogen transfer and hydrogenation, dehydrogenation of alkanes, Suzuki biaryl coupling, Heck olefin arylation, and of course polymerization. Van Koten and coworkers applied multimetallic pincer compounds as Lewis-acid catalysts in the double Michael reaction between methyl vinyl ketone and ethyl α-cyanoacetate and modified ruthenium pincer complexes (Scheme 5). Furthermore, van Koten and coworkers also proved the usability of pincer complexes in the field of sensors and switches [29-31]. More fundamental is the catalytic single bond activation of C–X (X = C, N) bonds using PCP and PCN complexes [32].

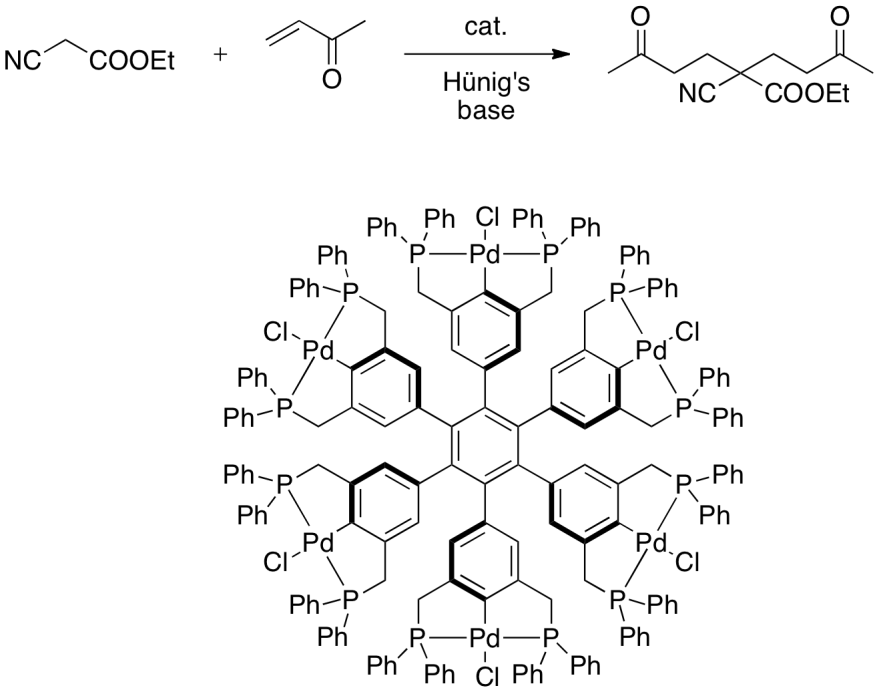

Scheme 5: Double Michael addition catalyzed by multimetallic palladium PCP complexes [32].

10 Hydrogenation

10.1 Introduction

Almost as important as the hydrogenation of C=C bonds is the hydrogenation of C=O bonds, since they are present in the most abundant starting materials. β-ketoesters are readily available via various condensation products and aryl alkyl ketones are usually easily accessible via Friedel-Craft acylation. Due to their prochirality it is easy to produce enantiomerically pure alcohols via enantioselective homogenous catalytic methods. Further chemo-, and enantioselective reduction of unactivated ketones is still a big problem. The first attempts to face this problem were the use of a stoichiometric amount of chiral metal hydrides or chiral boron reagents [33]. Particular effective are Ru(II) complexes of the type *trans*-[$RuCl_2$(BINAP)(DAIPEN)] (Scheme 6). This catalytic system has almost enzyme like properties with high turn over numbers (TON) of about 10^6 at a high turn over frequency (TOF) at room temperature exceeding an *ee* of 95% [6,34].

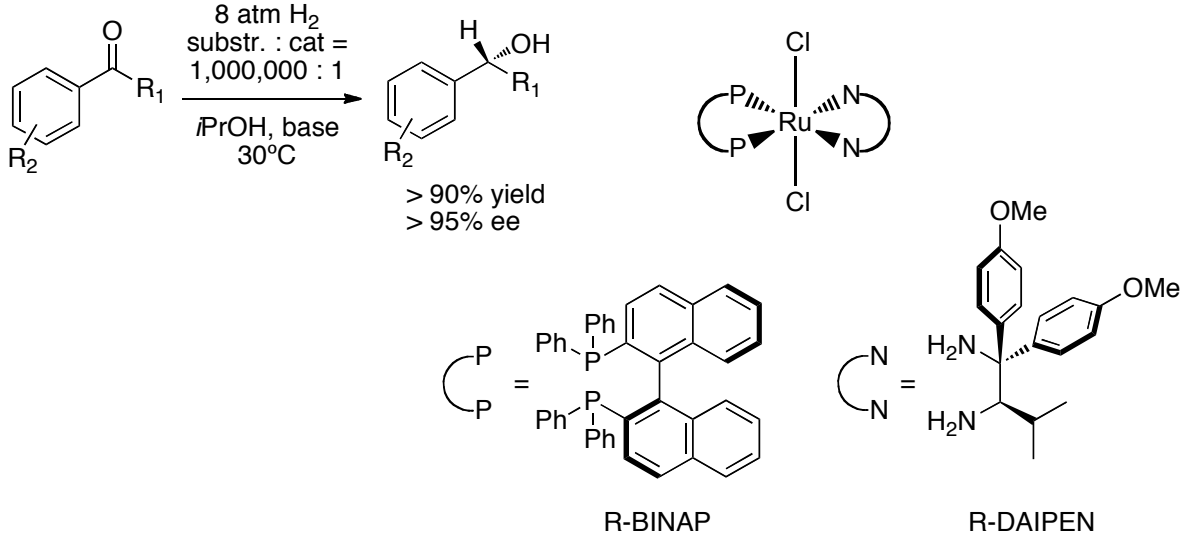

Scheme 6: Noyori's catalyst (*trans*-[$RuCl_2$(BINAP)(DAIPEN)]) for the reduction of unactivated ketones, using R-BINAP, and R-DAIPEN as chiral ligands [6,34]

Still, the most effective and mainly used complexes are those bearing platinum metals as a core atom [6,35]. The problem, which arises by using these rare and precious metals, is their toxicity and of course their prohibitive price, which is a huge drawback for industrial, and large-scale use [36]. Therefore the substitution by iron compounds is a necessity of nowadays research of organometallic- and inorganic chemistry, which makes this field “greener” and more sustainable. Iron is the 4th most abundant element in the earth crust, and therefore ubiquitously available, inexpensive, and environmentally benign. Furthermore it is non-toxic, and a positive side effect is that it is essential for the human body contrary to the elements used in catalyses nowadays. Moreover, many iron salts are readily available, or published in the literature [35-37]. Albeit iron is very cheap and easily accessible the field of iron catalysis is fairly young, and recently growing. Lately there have been remarkable milestones especially in the field of hydrogenation, which will be elucidated in this chapter.

10.2 Overview

Hydrogenation with precious metals, especially ruthenium based catalysts, is a well-known principle. The vast majority of publications deal with the optimization of metal and ligands systems to enhance the TON at a good TOF, the yield, the enantioselecitvies, and so forth. When considering the pioneering work performed in the field of ligand development (*vide* 9.1 Overview) as far as hydrogenation using iron catalysts is concerned, a scarcity of results is evident in the literature. Only in the last decade there is an increasing interest in iron chemistry, due to its low costs and sustainability.

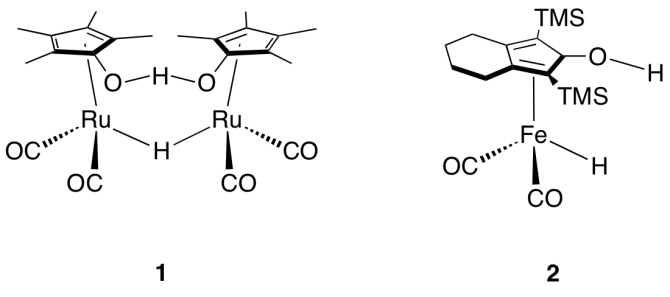

1 **2**

Figure 7: Model of Shvo’s ruthenium catalyst and Knölker’s / Casey’s iron catalyst as active hydrogenation catalysts.

The first efficient iron catalyst, which was used for the reduction of ketones, was reported by Casey and Guan in 2007 [6]. During their investigation of a tolyl analogue of the active reducing agent of Shvo's ruthenium catalyst (Figure 7) [38], they took in account that it should be possible to use Knölker's iron complex [39], which shows certain similarities to Shvo's catalyst, as an active hydrogenation catalyst for an acidic hydrogen transfer to carbonyl compounds [40]. The ruthenium catalyst **1** is able to reduce 1880 equivalents of neat acetophenone with 35 bar H_2 at 145ºC in 4.3 h (the average TOF is 423 h^{-1}). On the contrary Casey converts 42 equivalents with 3 bar H_2 at 25ºC in 20 h (with an average TOF of 2.1 h^{-1}) [6]. It is evident that the performance of the iron catalyst is lower than the ruthenium catalyst, but the reaction conditions are far milder than for the ruthenium analogue and therefore the results are remarkable. Shvo provided evidence that this hydrogenation precedes via an outer sphere mechanism (Scheme 7). In the first step a hydrogen transfers from the hydroxyl group of the cyclopentadienyl ligand and the metal hydride to the carbonyl bond of acetophenone, which is immediately reduced to 1-phenylethanol. In the second step hydrogen splits heterolytically and forms the starting complex **1**. This catalytic cycle is supported by the fact, that ketones are selectively reduced in presence of non-polar olefins [6].

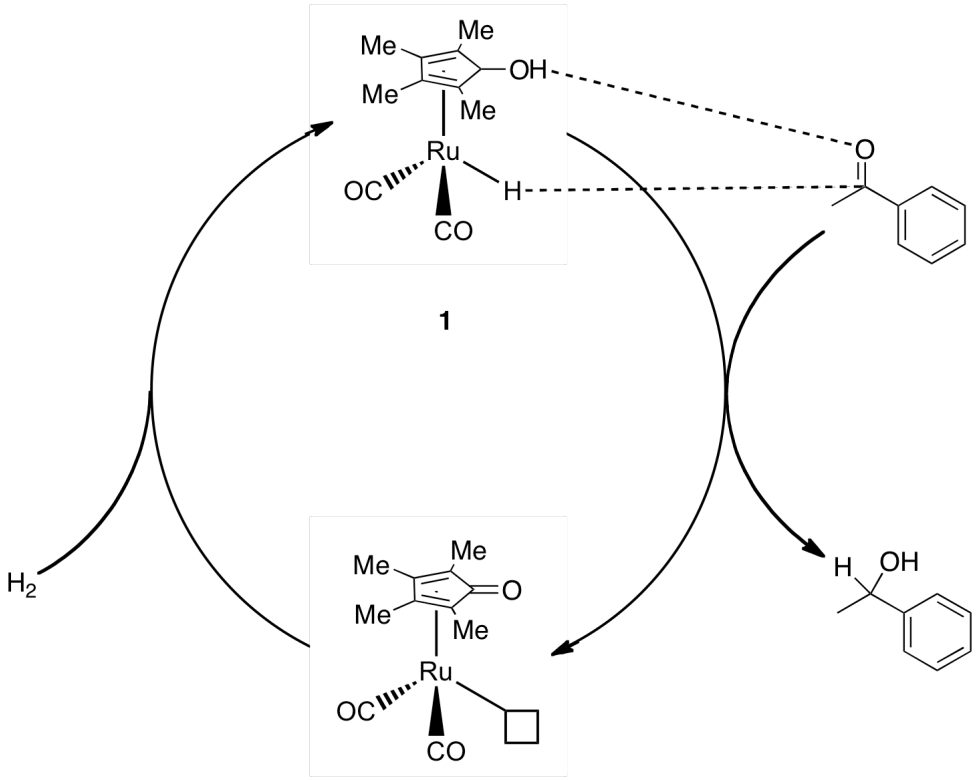

Scheme 7: Catalytic cycle of the active species of Shvo's catalyst [38].

Due to the close relationship of Shvo's and Casey's catalyst, Casey expected a similar catalytic cycle as the previous, shown in Scheme 7. They were able to show that in the absence of H_2 acetophenone and acetone form an iron-alcohol complex. Complex **2** (Figure 7) showed in the presence of the asymmetrical acetophenone two ^{1}H NMR resonance signals for the diastereotopic TMS group, while only one single signal was observed in the case of symmetrical acetone (Complex **4**) (Scheme 8). Unfortunately it was not possible to isolate and characterize these structures since the conversion of the ketone is not complete and the complex decomposes to an unknown product and the reduced alcohol (1-phenylethanol or *iso*-propanol). Different approaches using benzaldehyde as carbonyl source lead to an isolable iron-benzyl alcohol complex, which was characterized by XRD. These complexes were furthermore studied for their kinetic and thermodynamic stability towards substitution reactions. They also investigated the hydrogen transfer of **2** to aldehydes using inter- and intramolecular alcohol trapping agents, such as triphenylphosphine, pyridine, and benzonitrile [41].

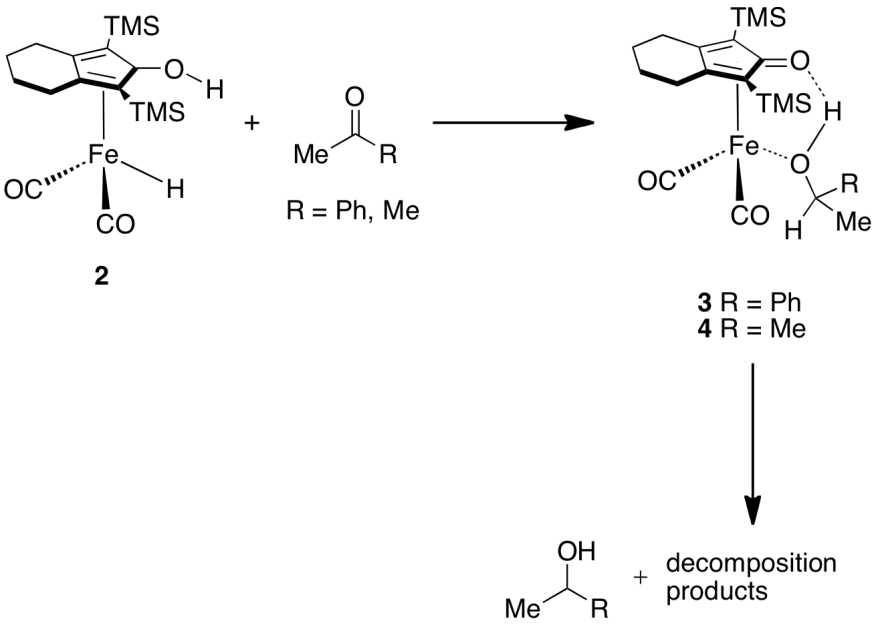

Scheme 8: Reaction of ketones with Casey's catalyst in the absence of H_2 [41].

These results support the evidence that the reduction of carbonyls operates via an concerted addition mechanism, which involves the Fe-H and cyclopentadienyl-OH hydrogen atoms outside the metal coordination sphere, but it is still difficult to determine whether these complexes are intermediates in the catalytic process or not. For further understanding of this catalytic process, Zhang and coworkers performed DFT calculations on experimental data, which was observed by Casey and Shvo, in order to elucidate the catalytic intermediates, which are formed during the hydrogenation process.

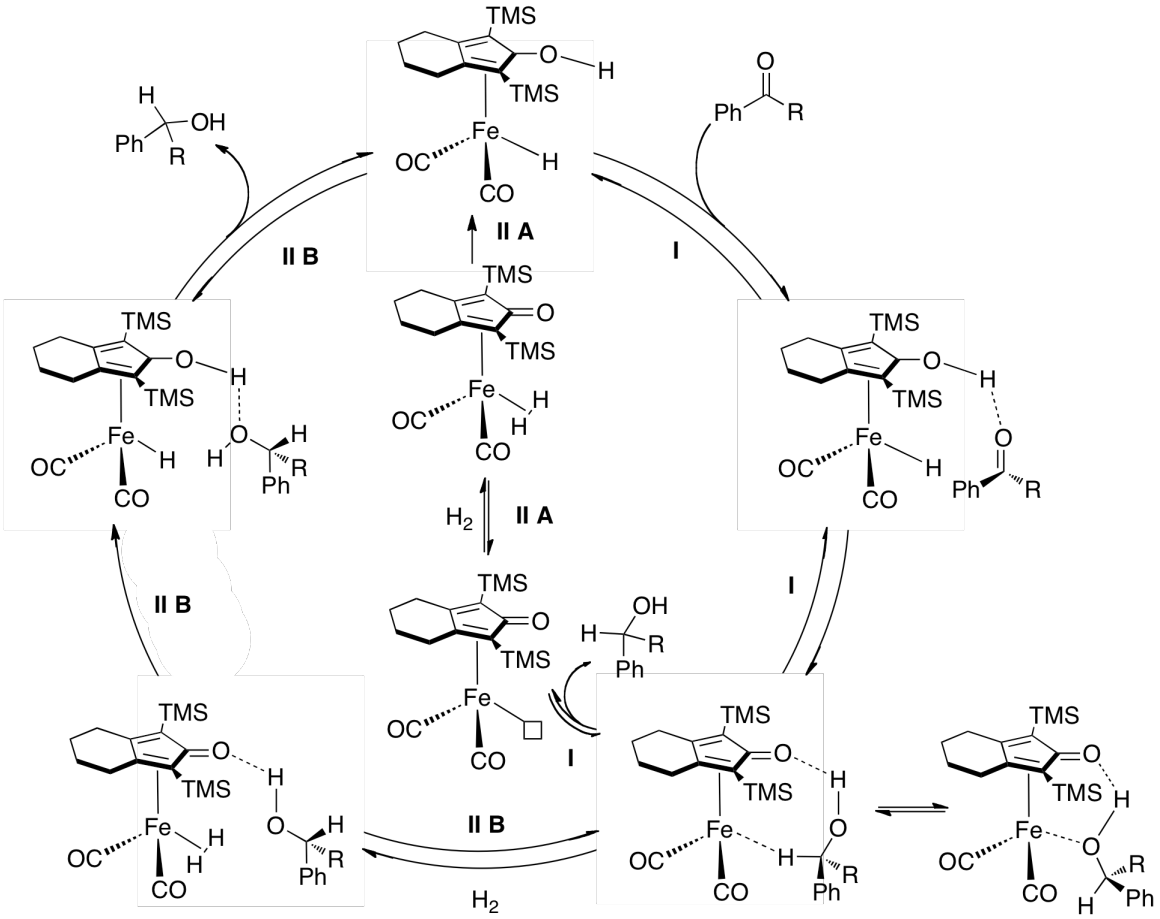

Scheme 9: Catalytic cycle proposed by Zhang and coworkers, which based on DFT calculations [42].

In Scheme 9 there is the detailed catalytic cycle of benzaldehyde and acetophenone. This cycle is divided into two parts. The first part is the hydrogen transfer process, which proceeds via a metal-ligand bifunctional mechanism. The hydrogen transfer comprises a concerted transfer of hydrogen atoms, which are attached to the metal center and the oxygen atom – which itself is linked to the cp ligand – to the carbon and oxygen of the carbonyl.

The second part is the regeneration of the catalyst, which takes place via a heterolytic splitting of H_2 molecules. This process in general has been proposed to occur facilitated in the presence of alcohols. Zhang investigated two reasonable pathways. One considers the splitting of H_2 without (Path “II A”) and the other with the participation of the alcohol molecule (Path “II B”). The conclusion of the work was that the iron-alcohol complex was the most stable of

the species considered in those calculations. For the two pathways of the hydrogen activation process with and without the participation of the alcohol molecules, both are starting the same way, by coordinating H_2 molecules as an unsaturated iron intermediate forming an stable η^2-H_2 complex. The calculation indicated that the activation barrier is significantly lowered by the mediation of alcohols. The rate-determing step is transfer of the hydrogen (I) to the carbonyl.

More recent was the work done by Gao and coworkers. Since the mid 1990's his group was working on chiral P_2N_2 and $P_2(NH)_2$ ligands (Figure 7) and their use in asymmetric transfer hydrogenation using ruthenium, iridum and rhodium as metal core of the catalyst. These ligands consist of a 'hard' nitrogen donor side and a 'softer' phosphorous donor side. They are usually perpendicular to each other and restrict the geometry on the metal center [43]. Gao had strikingly good results by using different iridium, ruthenium, and rhodium metal precursors. Lately they reported in a chinese journal the asymmetric transfer hydrogenation using an iron cluster and an enantiomerically pure P_2N_2 ligand with very good conversions and *ee*'s up to 98%. Based on IR-spectroscopic data Gao claimed that the iron cluster stays intact during the catalysis [4,44-49].

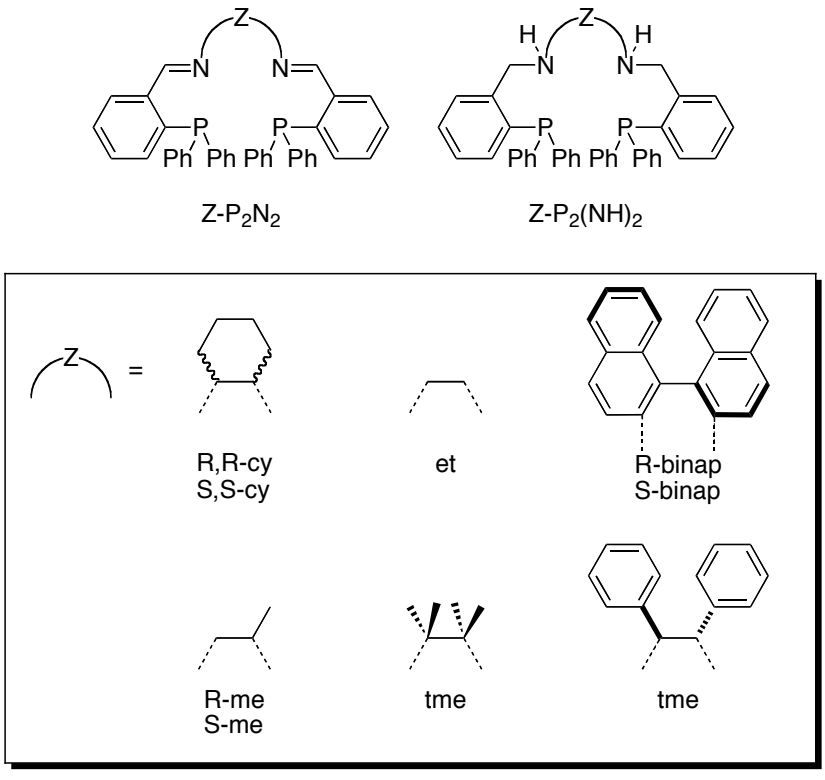

Figure 8: Gao's and Morris' P_2N_2 and $P_2(NH)_2$ ligand [43-48]

Later on Morris and coworkers used this concept of P_2N_2 and $P_2(NH)_2$ complexes on asymmetric hydrogenation. The first attempts based on ruthenium catalyzed hydrogenation of ketones [50]. Later on they transferred these ligands to iron based precursors and performed hydrogenation and transfer hydrogenation with those iron P_2N_2 and $P_2(NH)_2$ complexes. The results were remarkable. The rates are already competitive to for example Noyori's *trans*-[$RuCl_2$(BINAP)(DAIPEN)] catalyst, which is widely used for hydrogenation.

10.3 Mechanism

In Scheme 9 it is apparent that the hydrogenation divides basically into two parts; hydrogen transfer of the complex to the carbonyl compound and the catalyst regeneration *via* heterolytic dihydrogen splitting.

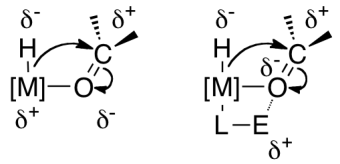

Figure 9: Inner sphere mechanism.

Homogenous transition metal catalysis usually involves the reactants forming products while they are somehow bonded to the metal center of the complex. In the case of carbonyl compounds it is generally assumed that the polar bond, which is reduced by the metal hydride complexes, is coordinated to a vacant coordination side of the metal complex, which was previously occupied by a different easily dissociable ligand. The coordination takes place in the inner or primary coordination sphere of the metal center. This bonding allows the electrophilic activation of the carbon of the polar carbonyl compound to enable the hydride, which is located in the *cis* position, to migrate to this carbon located in a β-position to the metal (Figure 9, left mechanism). Those kinds of mechanisms are called inner sphere mechanisms. They are usually identified by dissociation of ancillary ligands, to produce a vacant coordination site for the

substrate [51]. The electrophilic metals usually tend to form σ-complexes rather than π-complexes with the carbonyl compounds. The delivery of the hydride from the metal center to the carbonyl carbon is difficult due to geometrical reasons. The required interaction between the metal hydride and the π-face of the carbonyl is only achieved through drastic geometric changes of the σ-structures [52]. In some instances a coordinated ligand, which normally contains an electrophilic hydrogen bond donor group provides additional activation for the polar bond towards the hydride transfer (Figure 9, right mechanism) [51]. The weak point of the inner sphere hydrogen transfer is that the resulting alkoxide may undergo the reverse reaction – β-elimination reaction – unless it is rapidly cleaved off under formation of new hydride species.

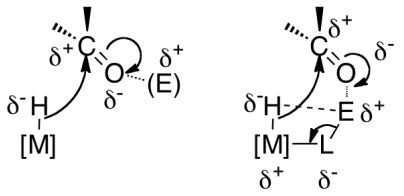

Figure 10: Outer sphere mechanism.

Noyori did some seminal work on the description of the non-classical reduction. These mechanisms are proposed to work in the second – outer – sphere of the metal center, by direct reduction of the carbonyl to the alcohol, without the intermediate of an alkoxide – *vide supra* –. The carbonyl carbon usually has a low hydride affinity; therefore an electrophilic activation is required. Those electrophiles are either from an external molecule, or internal from an ancillary ligand (Figure 10) [51,52].

10.4 Formation of the Hydride

In the formation of hydrides, hydrogen gas is usually the first gas, which coordinates to a vacant side on the metal core as an η^2-dihydrogen ligand. In Scheme 10 there are several possibilities for the coordinated dihydrogen to form a hydride. In path **A** an external nucleophile polarizes the dihydrogen bond, which leads to a heterolytic splitting, forming a metal hydride and a protonated base. Path **B** shows an intramolecular attack by a nucleophilic substituent of an ancillary ligand, leaving behind a protonated ligand. The third possibility is shown in path **C**, which shows a homolytical splitting of the coordinated dihydrogen molecule with a further oxidative addition to the ruthenium core atom, leaving behind an oxidized dihydride species [51,53].

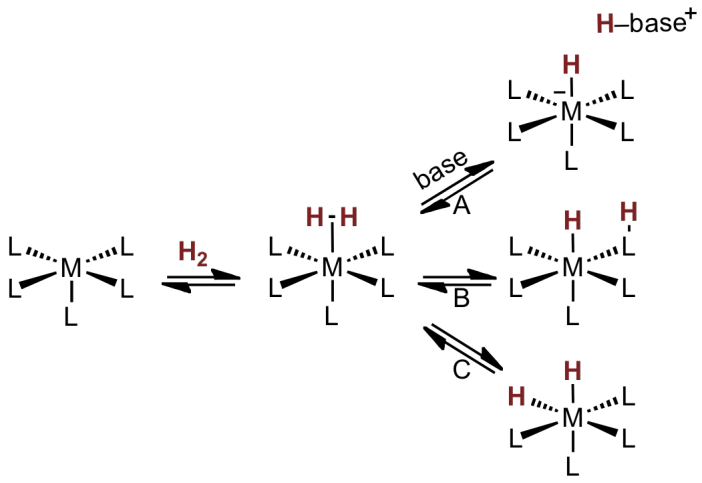

Scheme 10: General scheme for hydride formation.

11 Results and Discussion

11.1 General

In the last decade our group gained a lot of experience in the field of pincer complexes – *vide supra* –. We were able to synthesize various PNP and PCP type pincer complexes exhibiting several precious metals like ruthenium, palladium, platinum, and of course also non-precious metals like molybdenum and iron [25,54-57]. Using iron lead to strikingly good results at the stereo selective coupling of diazoacetates with aromatic aldehydes (Scheme 11), such as benzaldehyde derivatives forming exclusively 3-hydroxy-2-phenylacrylate in very good yields. Unlike the conventional way, using a lewis acid, like $AlCl_3$ or $SnCl_4$, which forms almost exclusively 3-oxo-3-phenylpropanoate.

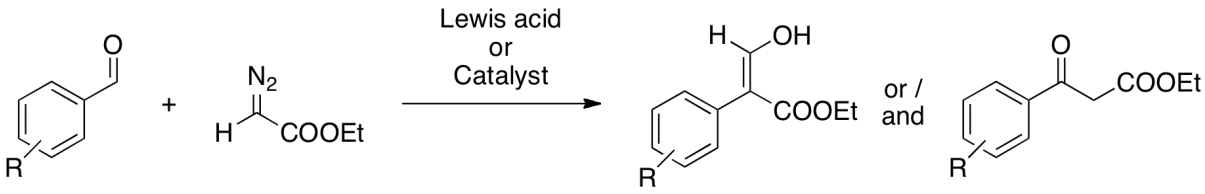

Scheme 11: Cross coupling of a benzaldehyde derivative with diazoacetate using various iron-PNP complexes [57].

Further research about catalytic applications of the iron pincer complexes lead us to the point to use these complexes in the field of hydrogenation and transfer hydrogenation. Since the electron donating properties of the pincer ligands are very supportive for hydrogen transfer of an hydride complex to carbonyl compounds [51]. This idea was also supported by the work of Morris and coworkers, who recently used their well-known P_2N_2 ligands (Figure 8) in combination with various iron precursors [3,5,6]. They managed to reach good TON's in hydrogenation and transfer hydrogenation, which are seriously

competitive with normal ruthenium based hydrogenation catalysts. These results encouraged us to use our existing non-chiral iron-PNP complexes to screen them for their activity in hydrogenation and transfer hydrogenation and also to try to develop new ligands in order to perform enantioselective reduction of carbonyl compounds. The complexes, which were used for the hydrogenation, are listed in Figure 11.

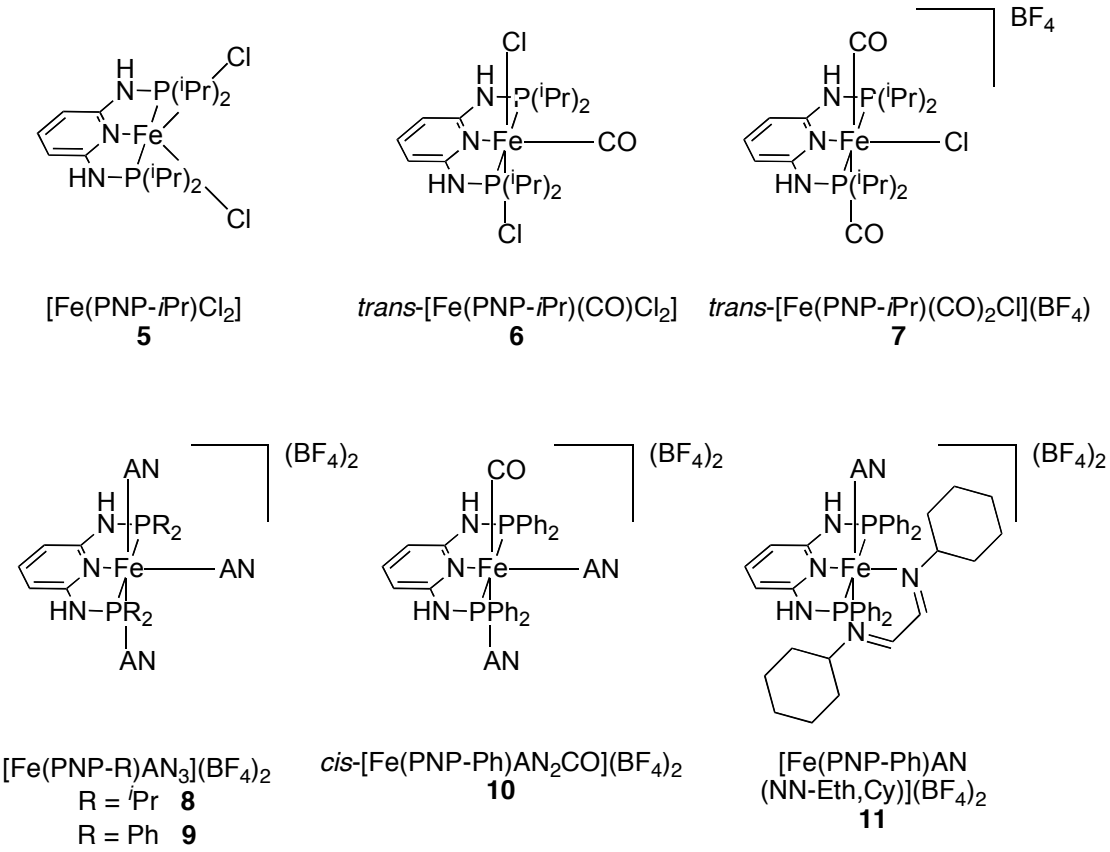

Figure 11: List of complexes used for hydrogenation.

11.2 Reaction Conditions

The substrate for the first screening experiments was acetophenone, which was reduced to 1-phenylethanol. The hydrogenations were carried out with 5% catalyst and 25% base loading at a temperature of 30ºC and 30bar H_2 pressure.

The choice of the right solvent is crucial for the hydrogenation, and depends on a number of factors such as the substrate being reduced, the catalyst, and, of

course, temperature and pressure [9]. It is important that the educt, the formed products, the catalyst, and all intermediates formed during the reaction, are soluble in the solvent system. Furthermore the acidity and basicity of the solvents, which is usually accounted for by the different donor and acceptor numbers of solvents, have a huge influence on the rate and selectivity of the reaction [58]. The solvents used for hydrogenation are listed in Table 1. These were screened in the hydrogenation of acetophenone using complex **6** (Figure 11) as catalyst.

Table 1: Variation of Solvents.

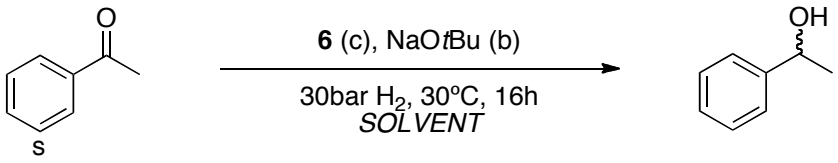

c(s) = 0.2 mol*L^{-1}
c:b:s = 1:5:20

No	Solvent	Yield [%]
1	Methanol	1.9
2	Ethanol	98.9
3	*iso*-Propanol	14.5
4	DCM	0.0
5	Acetone	N/A
6	THF	31.4
7	THF	99.4*

* Reaction at 50°C

In Table 1 it is evident that methanol, *iso*-propanol, DCM, dioxane, and THF – at 30ºC – (entries 1, 3, 4, 6, and 8) lead to a fairly low or no conversion, while acetone (entry 5) lead to the formation of several intractable side products. In this case no evidence for the desired product was obtained. It is very probable that in this case due to the high base concentration some kind of condensation reaction occurred. Only ethanol (entry 2) and THF (entry 7) at the elevated temperature of 50ºC lead to almost quantitative conversion. Since ethanol catalyzes the reaction at lower temperatures it was used for further screening.

The next step was to investigate if the amount of base could be lowered without loss of conversion. Müller and coworkers made a wide spread screening based on the seminal work done by Walling and coworkers, which were able to show that at certain H_2 pressures and temperatures base catalyses the hydrogenation of carbonyl compounds without the presence of transition metal catalysts [59,60]. To prove that base catalyzed hydrogenation does not occur blank tests were performed (see Table 2).

Table 2: Variation of base concentration.

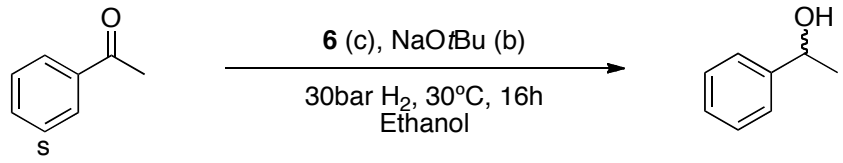

c(s) = 0.2 mol*L^{-1}
c:b:s = 1: *1-5* :20

No	Ratio (c:b:s)	Yield [%]	Yield (blank test) [%]
1	1:1:20	0.4	0.0
2	1:2:20	10.9	0.0
3	1:3:20	26.1	0.0
4	1:4:20	53.5	0.0
5	1:5:20	98.9	0.8

Table 2 shows that the conversion is equally increasing with the amount of base with a peak at 25% base loading (entry 5). Even though there was a slight turn over noticeable at the blank test we moved on using 25% base loading.

Before screening for the optimal base we wanted to know whether instead of using an alkoxide base it was possible to activate the complex with a nitrogen base like pyridine or Hünig's base (*N*,*N*-diisopropylethylamine). Therefore **6** was suspended in d_8-THF and the bases were added. Since there was no change in solubility, color, and shift in the ^{31}P NMR spectrum it is evident that there is no activation by nitrogen bases. Further screening was performed using alkoxide bases as shown in Table 3 (entries 1 – 5). For comparison the base loading was

reduced to 20%. Of all the bases tested NaO*t*Bu (Table 3, entry 2) gave the best results.

Table 3: Variation of bases.

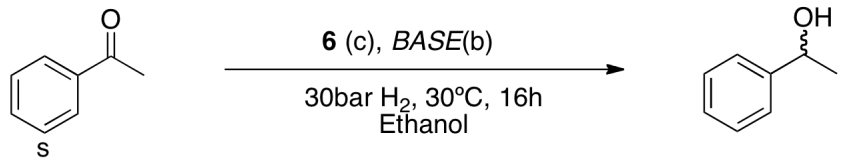

c(s) = 0.2 mol*L^{-1}
c:b:s = 1:4:20

No	Base (b)	Yield [%]
1	LiO*t*Bu	7,9
2	NaO*t*Bu	50,4
3	KO*t*Bu	36,2
4	NaOMe	7,2
5	NaO*i*Pr	5,9

11.3 Hydrogenation

Further considerations about the right solvent led us to use THF as the solvent of choice. THF is a non-protic solvent, which will not react with the base. In this solvent almost quantitative conversion at 50ºC was found (Table 1, entry 7). Complexes **5** to **11** (Figure 11) were then screened in the hydrogenation of acetophenone using THF and 30bar H_2 pressure at 50ºC. The results are depicted in Table 4. It has to be noted that complex **5** was insoluble in THF after the addition of base and no catalytic reaction took place.

Table 4: Hydrogenation of Acetophenone.

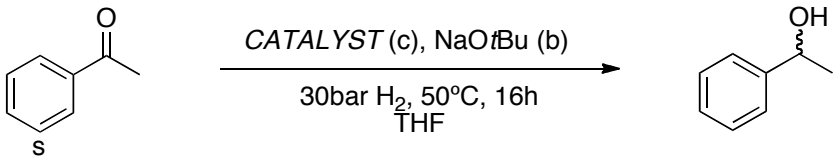

c(s) = 0.2 mol*L^{-1}
c:b:s = 1:5:20

No	Catalyst (c)	Yield [%]
1	*trans*-[Fe(PNP-*i*Pr)(CO)Cl_2] (**6**)	99.4
2	*trans*-[Fe(PNP-*i*Pr)$(CO)_2$Cl]BF_4 (**7**)	0.0
3	[Fe(PNP-*i*Pr)AN_3]$(BF_4)_2$ (**8**)	0.0
4	[Fe(PNP-Ph)AN_3]$(BF_4)_2$ (**9**)	1.9
5	*cis*-[Fe(PNP-Ph)(CO)AN_2]$(BF_4)_2$ (**10**)	11.1
6	[Fe(PNP-Ph)AN(NN-Eth,Cy)]$(BF_4)_2$ (**11**)	0.0

Complexes **7**, **8**, and **11** (entries 2, 3, and 6) did not show a good catalytic performance. In the case of complex **7** (entry 2) there was a change of color noticeable after the addition of the base indicating that the base reacts with the complex forming probably an alkoxide complex instead of a chloride complex – *vide infra*. This base deactivated complex turned out to be catalytically inactive.

For complexes **8** and **9** (entries 3 and 4) the conversion is very low, even though these complexes are structurally similar. The slight difference is explainable with the electron density at the phosphorous atom. The inductive effect of the aliphatic *iso*-propyl groups is lower compared to the phenyl groups. Therefore the phosphorous atom linked to the phenyl groups is a stronger donating ligand compared to the other one bonded to the *iso*-propyl group [56,57]. This induced a higher electron density at the metal center, which is supportive for hydrogenation because of the positive charge, which remains after the hydrogen transfer from the metal center to the carbonyl (*vide* 10.3 Mechanism) [51]. Complex **10** confirms this theory (entry 5), where a carbonyl is positioned *trans* to the leaving acetonitrile ligand, which cleaves off for hydrogenation. The electron density at the metal core is again increased, which yields in a higher reaction rate.

In the case of complex **10** (entry 6) no reaction took place presumably for steric reasons (Figure 18; *vide* 13.3.1 PNP-Complexes). This complex was developed to mimic the substitution pattern of the P_2N_2 ligands. Therefore **11** was expected to be capable of performing an outer sphere hydrogenation mechanism with the assistance of the ancillary diimine-ligand. To overcome this problem it might be useful to reduce the bulkiness of the diimine ligand.

The only complex, which exhibited good results was complex **6** (entry 1). A plausible hydrogenation mechanism is proposed in the next chapter (*vide* 11.4 Mechanistic Studies).

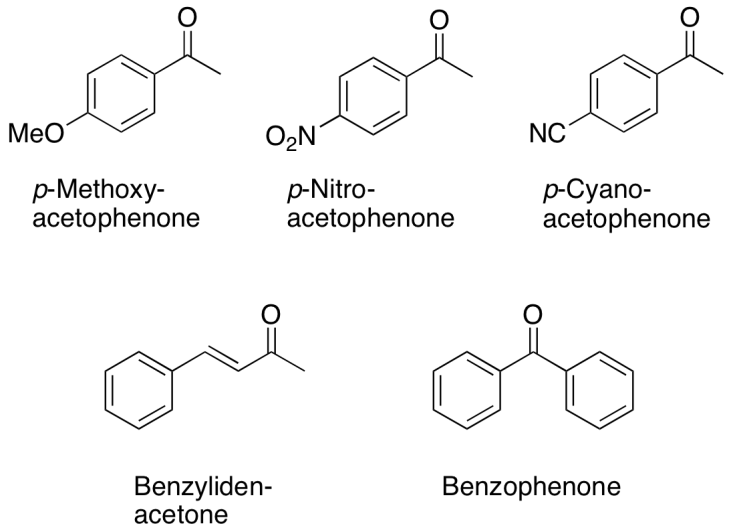

Figure 12: Further substrates to check for chemoselectivity of complex 6.

Furthermore, different substrates (Figure 12) were screened in order to test complex **6** for its chemoselectivity and reactivity. These results are listed in Table 5. To make it easier to compare the conversions of the different substrates the temperature and the hydrogen pressure were reduced to 40ºC and 25 bar H_2.

Table 5: Hydrogenation of various substrates.

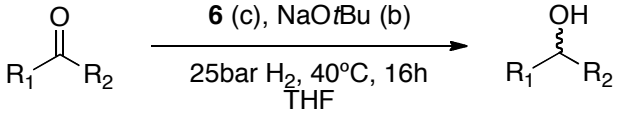

s

c(s) = 0.2 mol*L^{-1}
c:b:s = 1:5:20

No	Substrate (s)	Yield[a] [%]
1	Acetophenone	96.2
2	*p*-Methoxyacetophenone	33.1
3	*p*-Nitroacetophenone	19.1
4	*p*-Cyanoacetphenone	26.0
5	Benzylidenacetone	N/A[b]
6	Benzophenone	0.0

[a] The yield was determinded by NMR spectroscopy using a 250 MHz Bruker NMR spectrometer.

[b] Due to the high base concentrations various aldol condensation products were observed, which have not been further investigated.

The substrates can be subdivided into reference material (entry 1), substrates with electron donating (ED) substituents (entry 2), substrates with electron withdrawing (EW) substituents (entries 3, and 4), substrates with different functional groups (entries 4, and 5), and non-enolizable substrates (entry 6). The activating and deactivating substituents on the acetophenone derivatives were positioned *para* to the carbonyl group to avoid steric hindrance during the catalytic reaction.

As expected the *p*-methoxyacetophenone showed a lower conversion. The reason for this may be its ED properties, which increases the electron density on the carbonyl carbon making it less electrophilic. Therefore, the rate of the nucleophilic attack by the hydride, which leads to an oxidative addition on the carbonyl carbon, is lowered. This theory is also approved by the literature, where using methoxy substituted always yielded in a lower conversion [61].

In the case of EW substituents we expected a better conversion than due to an increasing of the electrophilic character of the carbonyl carbon, which is also approved by literature [40,61]. In Table 5 it is evident that the conversions are against this expectations lower. The reason for this might be that the other polar functionalities on the aromatic ring interact with the metal center, which makes it less active for further hydrogenation. This theory might be confirmed by simply taking a halide derivative instead. The halide mimics the same properties – in terms of EW effect – like the cyano- and nitro substituent, but does not further interact with the metal center.

The substrates in entries 4 and 5 were taken to check the chemoselectivity of the catalyst towards nitriles and double bonds. The crude NMR of the *p*-cyanoacetophenone showed only reduced alcohol besides the starting material, which shows a good chemoselectivity against nitriles. The hydrogenation of benzylidenacetone yielded in no reasonable results. The reason for this might be the high base concentration, which led to a series of different condensation products, but those have not been further investigated.

In the case of benzophenone (entry 6) the hydrogenation showed no result. The reason for this can be versatile. The most plausible one is explainable due to the electrophilicity of the carbonyl bond. Since benzophenone has two strong inductive donating groups, the electron density at the carbonyl bond is way higher than in comparison with acetophenone. This makes this bond less attractive for a hydridic attack whilst bonded to the metal center. To double-check whether this is the problem or not it would be useful to take different non-enolizable ketones, such as hexamethylacetone, or 2,2-dimethylpropiophenone.

In conclusion, complex **6** gives an active catalyst with a good chemoselectivity towards nitrils. To determine the exact reactivity further work needs to be done to make it compatible to commercially used complexes.

11.4 Mechanistic Studies

During the investigations in hydrogenation we observed that complex **6** undergoes a change in solubility after the addition of base. Usually **6** is unsolvable in solvents such as Et_2O, hydrocarbons, and DCM, barely solvable in THF, and acetone, but good soluble in DMSO yielding a violet / blue solution. After addition of base it dissolves in all solvents mentioned above. UV/VIS spectroscopy revealed a shift of the absorption maximum from 578 nm [62] to 715 nm (blue to green). After addition of dihydrogen the solution turned orange. These color changes encouraged us to investigate the changes of the complex during the catalytic process by means of NMR and IR spectroscopy.

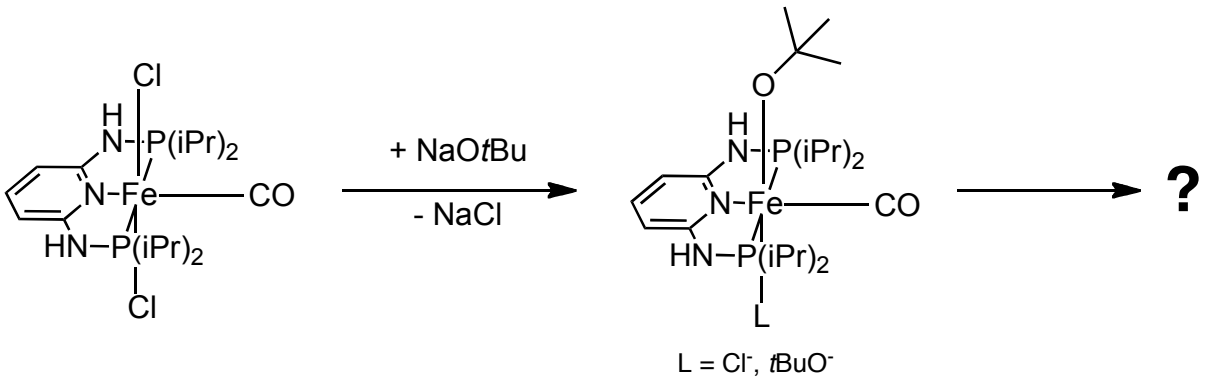

Scheme 12: Possible reaction scheme after the addition of base.

Adding base to a suspension of THF with **6** yields in formation of an intensive green solution, leaving back a white solid. In Scheme 12 it is proposed that one chloride ligand is replaced by a *tert*-butoxide anion thus eliminating sodium chloride. At this stage of the investigations it is still not clear whether one or two chloride ions get replaced. Furthermore the IR spectroscopy showed a shift of the carbonyl ligand from originally 1956 cm^{-1} [62] to 1617 cm^{-1}. This shift was also noticeable via ^{13}C NMR spectroscopy, where the carbonyl carbon shifted from formerly 224.81 ppm [62] upfield to 203.69 ppm. These drastic changes strongly point out that the nature of the coordinated carbonyl is changing towards a stronger shielding of the carbon atom. It is plausible that a base molecule attacks the electrophilic carbonyl, which probably forms a formate ester, but this proposal

is still rather tentative, and needs to be further investigated by NMR experiments and DFT calculations.

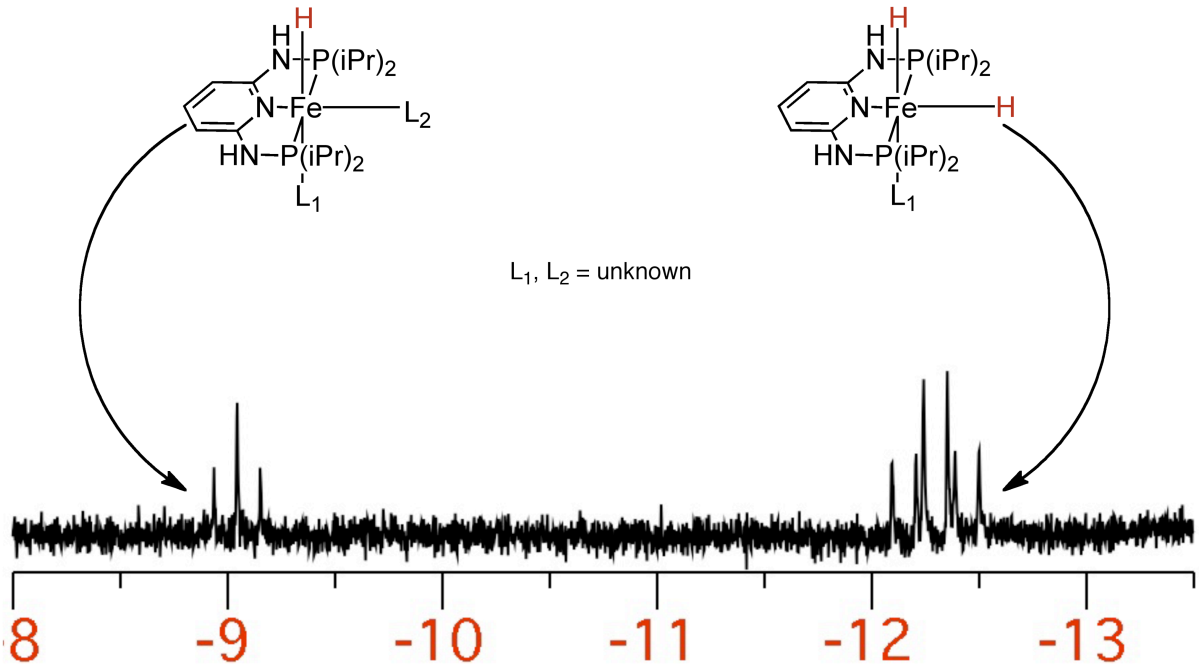

Figure 13: Evidence of hydride complexes.

After the introduction of dihydrogen to the activated complex solution two different hydride species were formed (Figure 13). They appear in a range of -8.5 ppm to -13.0 ppm. The triplet at -8.98 ppm was determined as a monohydride species. The coupling constant of 43.3 Hz derives from the coupling of the single hydride to the two phosphorus atoms ancillary to the central iron atom. The multiplet between -12.05 ppm and -12.46 ppm is built up by two triplets – with a coupling constant of 58.8 Hz and 58.6 Hz –, which are overlapping. The coupling system derives from two hydrides, which are coordinated to the metal center in a *cis* manner and *cis* with respect to the two phosphorous of the PNP ligand. The diamagnetism of this complex leads to the conclusion, that these complexes are still sixcoordinate with at least one CO ligand.

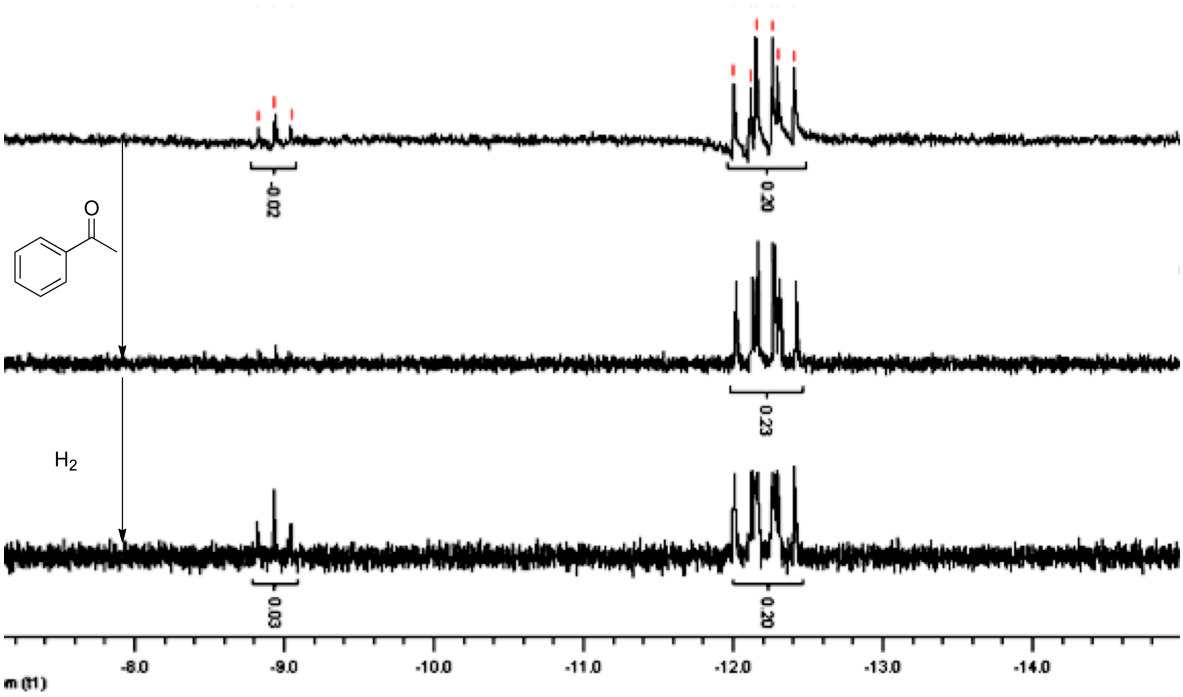

Figure 14: Catalytic activity of hydride complexes.

A further attempt was to look at the catalytic activity of these complexes. Therefore stoichiometrical amounts of acetophenone were added to the reaction vessel and the changes were monitored by ^{1}H NMR spectroscopy. In Figure 14 it is evident that only the monohydride species disappear after the addition of the substrate, while the dihydride species remains at the same concentration. After a further introduction of dihydrogen the monohydride species is again reformed. This leads to the conclusion that only the monohydride species is catalytically active, whilst the dihydride species does not participate in the catalytic reaction. Further investigations of this ^{1}H NMR spectrum revealed the complete reduction of the acetophenone to 1-phenylethanol, which points out the catalytic activity at room temperature with 1 bar dihydrogen pressure.

It is also interesting to see that the catalytic activity of this complex is higher than expected, since only about 20% of the catalyst participates at hydrogenation reaction.

To conclude this topic, we were able to point out interesting cornerstones of the catalytic cycle, which are interesting and crucial for the full understanding of this mechanism. In further work it is very important to fill up the voids – *e.g.* the

complete reaction mechanism of the base interacting with the catalyst, and the hydrogen interacting with the base-activated complex. In order to achieve this objective further NMR experiments have to be performed. After the exact mechanism from the starting complex to the hydride species is elucidated, it might be possible to change the parameters in such a way to that the formation of the catalytically inactive dihydride species can be avoided.

12 Transfer Hydrogenation

12.1 Introduction

There is a huge palette of different methods how to reduce carbonyl compounds, amongst them, the addition of hydrogen from a suitable donor molecule to a C=O bond receives increasing attention since the mid 90's of the last century. It has become one of the procedures of choice for the preparation of alcohols from ketones and – to a lesser extent – aldehydes. The use of transfer hydrogenation has many positive sides compared to conventional alternatives, which are available for the same transformation:

- operational simplicity,
- cheaper reagents compared to conventional methods,
- reduction of safety constraints associated with the use of gaseous hydrogen in high pressure vessels,
- less hazardous waste especially in the case of using metal hydrides – like boron, aluminum, and silicon hydrides – in stoichiometric amounts,
- safe, benign and low-cost reducing agents, and
- a large variety of metal catalysts of high activity and selectivity for the process [63].

12.2 General Overview

Transfer hydrogenation is basically very similar to hydrogenation itself; the main difference between those two types of reaction is the hydrogen source. Whilst hydrogenation methods use hydrogen gas as donor molecule, transfer hydrogenation uses various donor molecules, H_2D, like *iso*-propanol, formic acid in triethylamine, or sodium formate in an aqueous solution (Scheme 13). Those molecules donate hydrogen to the carbonyl in the presence of a suitable promoter – *e.g.* a transition metal catalyst – leaving back an oxidized side product, D.

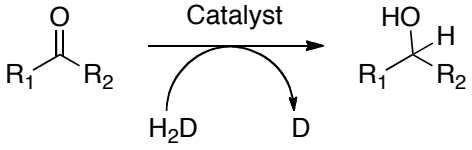

H_2D = *i*PrOH
HCOOH / Et_3N
HCOONa / H_2O

Scheme 13: General hydrogenation scheme.

The first examples of the reduction *via* hydrogen transfer of unsaturated organic compounds were published during the first decades of the last century [63-65]. An efficient approach for the reduction of carbonyl compounds were found in the mid 20's of the last century, when Meerwein, Ponndorf and Verley independently contributed their discoveries to the today well-known Meerwein-Ponndorf-Verley reduction (MPV-reduction; Scheme 14). The first report to appear in the literature was by Meerwein and Schmidt in 1925 [66], who showed that aldehydes could be reduced to the corresponding alcohol just by using $Al(OEt)_3$ in an ethanolic solution. Independently, Verley was able to show in the same year, that butyraldehyde could be reduced by geraniol in the presence of $Al(OEt)_3$ as base [67]. The year after, Ponndorf extended this reduction to include the reactions of ketones by using an easily oxidized, secondary alcohol, such as *iso*-propanol, as hydride source and $Al(O^iPr)_3$ as metal catalyst [68,69]. The key-step in this reaction is the six-membered ring as a transition state with a further rearrangement of the bonds. A decade later the reversibility of this reaction was exploited by

Oppenauer, who showed that this backward reaction allows a useful synthetic procedure for the oxidation of secondary alcohols in the presence of aluminum alkoxides and an excess amount of acetone, to shift the equilibrium to the side of the oxidized state of the starting alcohol [70].

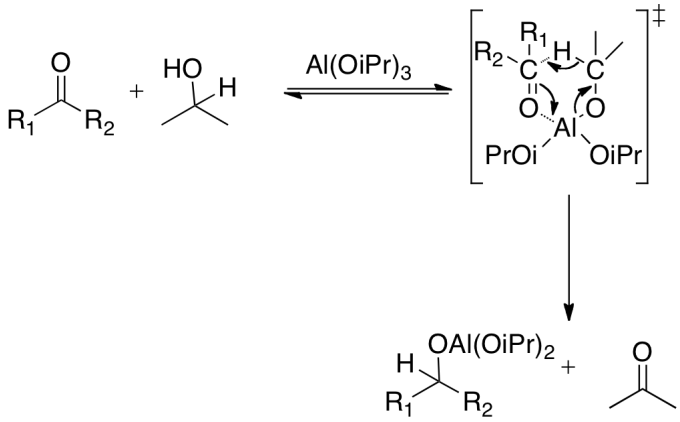

Scheme 14: General scheme for the Meerwein-Ponndorf-Verley reduction of carbonyl compounds.

The cornerstone for homogenous transfer hydrogenation was set in the 1960's by Bailar and Trocha-Grimshaw [71,72], who did some seminal work in the development of transition metal complexes and their further use in the reduction of ketones by hydrogen transfer. They used iridium-complexes for the reduction of cyclohexanones to the corresponding alcohol with *iso*-propanol as hydrogen donating molecule. This principle stayed in the dark until in the late 1970's Sasson and Blum gave it a renaissance. They were able to show that dichlorotris(triphenylphospine)-ruthenium-complexes showed good results in the transfer hydrogenation of acetophenone in *iso*-propanol [73,74].

Since then the way was opened to a wide field screening of symmetric and asymmetric ruthenium catalysts. Containing mainly chiral phopshine ligands. In the last decades the importance of this process as a synthetic tool for the reduction of ketones has grown steadily. Nowadays it can be seen as a competitive and successful method for the reduction of carbonyls [63].

The only drawback of this method to conventional hydrogenation methods is the production of the oxidized side product, D (Scheme 13), which can lead to a back reaction (similar to the Oppenauer oxidation), and the presence of the undesired side product that can make troubles in the further work up and isolation of the product.

12.3 Donor Molecules

In theory almost every compound, which is capable of transferring two hydrogen atoms under appropriate conditions can be taken as donor molecule. Albeit the most common and widely used molecules, which are able to perform metal catalyzed transfer hydrogenation, are *iso*-propanol, formic acid and its salts, since the by products are non-hazardous and easy to handle [63,75].

The use of *iso*-propanol as reductant is fairly common, due to its favorable properties; it is a cheap bulk chemical, it is stable, which makes it easier to store, it is easy to handle due to its moderate boiling point – 82ºC –, it is also non-toxic, which is a crucial point of nowadays chemistry, and it is easily disposable. The byproduct – acetone – is also easily separable due to their big difference of the boiling points, furthermore acetone is a very important precursor for the production of PMMA [76]. The weak point of *iso*-propanol is that the reduction is under thermodynamical control. It yields in a high conversion with a large excess of donor molecules. It is also compulsory to use alkali metal hydroxide or -alkoxide bases as a promoter to enable the alcohol to donate the hydrogen atoms to the desired carbonyl compound. Depending on the amount of base there is always the possibility of MPV-type reductions, which reduces the *ee* of the desired alcohol [63,75]

Formic acid and its salts are also well-known hydrogen-donating agents. They are well-behaving, and inexpensive [76]. The conversion of the carbonyls to the reduced alcohol is in this case kinetically controlled, since the formic acid is dehydrogenated to CO_2, and removed from the equilibrium, which makes this reaction irreversible, and leads, in principle, to a 100% conversion [75,76]. The

bigger advantage is that formic acid and their derivatives does not need strong basic promoters, they usually work with weaker bases such as triethylamine (TEA), which avoid the problem of unwanted side reactions. In the case of using formates the reaction can be taken out in water or in water-organic biphasic conditions, which is also a crucial point for organic synthesis, to make this field "greener" and sustainable. Albeit the use of formic acid derivatives are bringing a big advantage in terms of reactivity they also have a huge drawback, because of their inherent acidity that leads to a stronger interaction of the donor molecule with the metal center of the catalyst. In some instances this bonding can lead to an elimination of weakly coordinated ligands yielding in either deactivation, a loss of the chiral information, or complete decomposition of the catalyst. This makes formic acid incompatible with a large variety of active and widely used hydrogen transfer catalysts [63].

12.4 Mechanisms

The transfer of hydrogen from at donor molecule to a carbonyl can occur in different ways. The first one, but also most seldom one, is the direct hydrogen transfer from a hydroxy substituted sp^3-C atom, which is most likely from ethanol, 1-propanol, *iso*-propanol, but not methanol, to a sp^2-C of a carbonyl group. This reaction takes place under pure thermal conditions, without the help of any metal, basic or acidic catalyst. The transfer occurs *via* a six membered transition state with a further rearrangement of the bonds (Scheme 15). It is very rare, and more likely to occur with aryl and alkyl aldehydes but less likely with ketones [63].

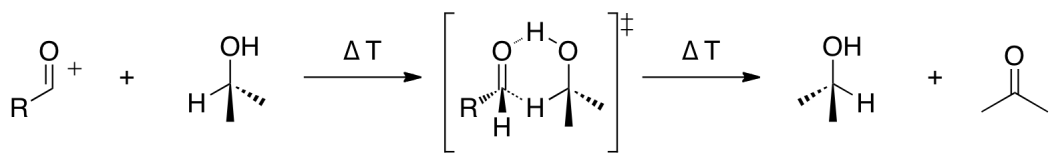

Scheme 15: Uncatalyzed concerted hydrogen transfer process.

In the presence of metal catalysts there are two different reaction pathways, the direct hydrogen transfer and the hydridic way. The direct route requires a simultaneously interaction of the carbonyl and the alcohol with the metal catalyst in a concerted process to form a six membered transition state similar to MPV-reduction mechanism (Scheme 14). Characteristic for this mechanism is the direct interaction of the donor and acceptor molecule without further formation of a hydride species. This mechanism is well-known for electropositive metals such as aluminum and lanthanides, but less common for transition metal complexes [63]. Zassinovich and coworkers reported this reaction mechanism for their iridium-diimin complexes [77], which was further proven by Handgraaf via DFT calculations [78].

The most common route is the forming of a hydridic intermediate of the metal catalyst with a further hydride transfer to the carbonyl carbon. A typical feature of the hydridic route is the formation of a metal hydride as the catalytic active species and the fact that the hydrogen donor and acceptor molecule coordinates separately to the metal center at different steps of the catalytic cycle [63]. The mechanism in general proceeds similar to the hydrogenation mechanism, which basically splits into two parts, the hydride transfer of the catalyst to the carbonyl, and the further regeneration of the catalyst leaving back the oxidized donor molecule. The reaction mechanisms are similar to those of the direct hydrogenation (Figure 9), and occur either *via* an inner or an outer sphere mechanism.

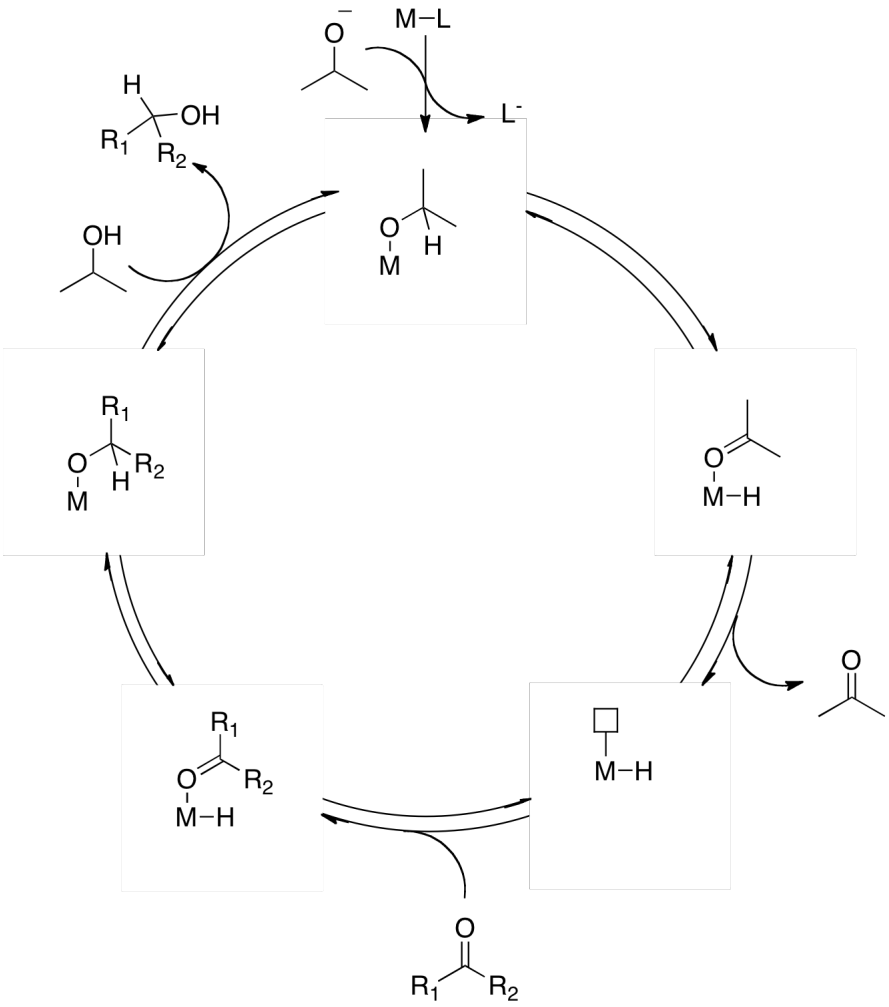

Scheme 16: Catalytic cycle following a inner sphere hydrogen transfer mechanism, using *iso*-propanol as donor molecule [51].

It is evident that in Scheme 16 the left hand side is mechanistically the same as in the inner sphere mechanism of the hydrogenation. The carbonyl coordinates to a vacant coordination side of the metal center perpendicular to the hydride. The next step is the *β*-addition of the hydride to the carbonyl carbon yielding the reduced carbonyl, which is further replaced by a donating molecule. The regeneration of the catalytic species takes place via the reverse *β*-elimination of the coordinated hydrogen donor [51].

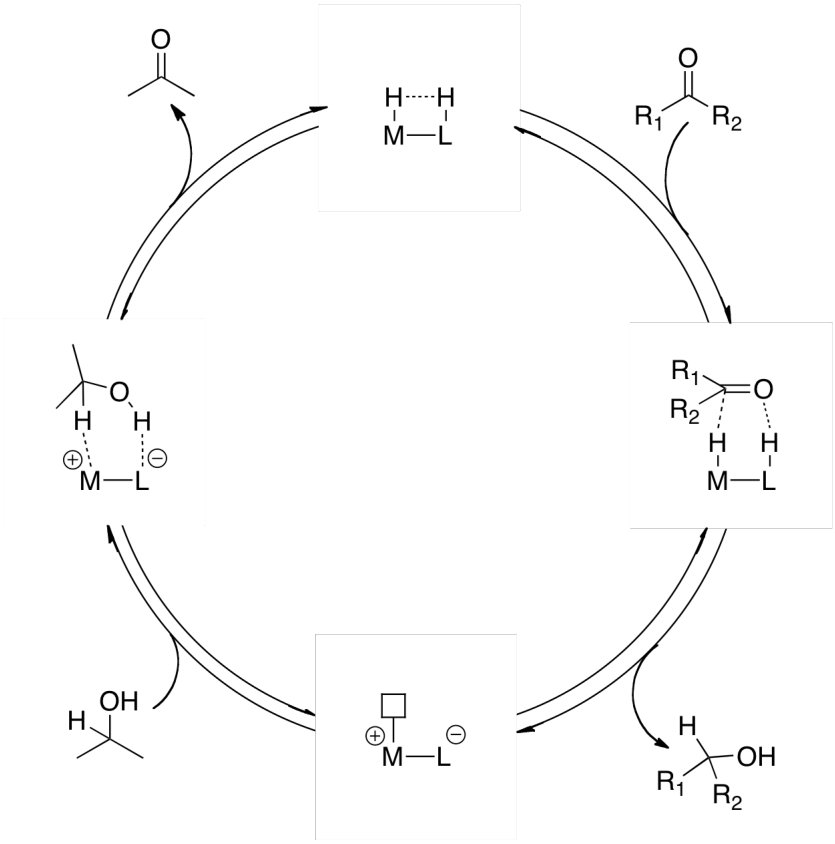

Scheme 17: Catalytic cycle following the outer sphere hydrogen transfer mechanism, using *iso*-propanol as donating molecule [51].

Noyori and coworkers have proposed the alternative pathway –the outer sphere mechanism –. In this case a chelating ligand with an amino group ancillary to the metal center bare a hydrogen atom *syn*-periplanar to metal hydride. Analogue to the outer sphere hydrogen transfer mechanism in the direct hydrogenation (Figure 10) the two hydrogen atoms at the metal center get transferred simultaneously to the carbonyl without forming a bond between the substrate and the metal center (Scheme 17). After the delivery of the hydrogen, the oxidized complex instantaneously dehydrogenate the donor species leaving back the starting complex [63,76].

12.5 Complexes

As already reported in a previous part of this chapter, the first catalytic approaches for the hydrogen transfer reaction were reported in the 1960's by Bailar and Trocha-Grimshaw [71,72] and further by Sasson and Blum in the 1970's [73,74]. Since then a large variety of different complexes, mainly basing on iridium, rhodium and ruthenium were developed. More recently even lanthanides, such as samarium, and gadolinium, gain increasing interest, since they are capable of performing a MVP-reduction type mechanism (*vide*, 12.4 Mechanisms) [63]. Since Noyori successfully used his *trans*-[$RuCl_2$(BINAP)(DAIPEN)] (Scheme 2) in transfer hydrogenation ruthenium is getting the metal of choice for the hydrogen transfer, it even outclasses iridium and rhodium (Figure 15).

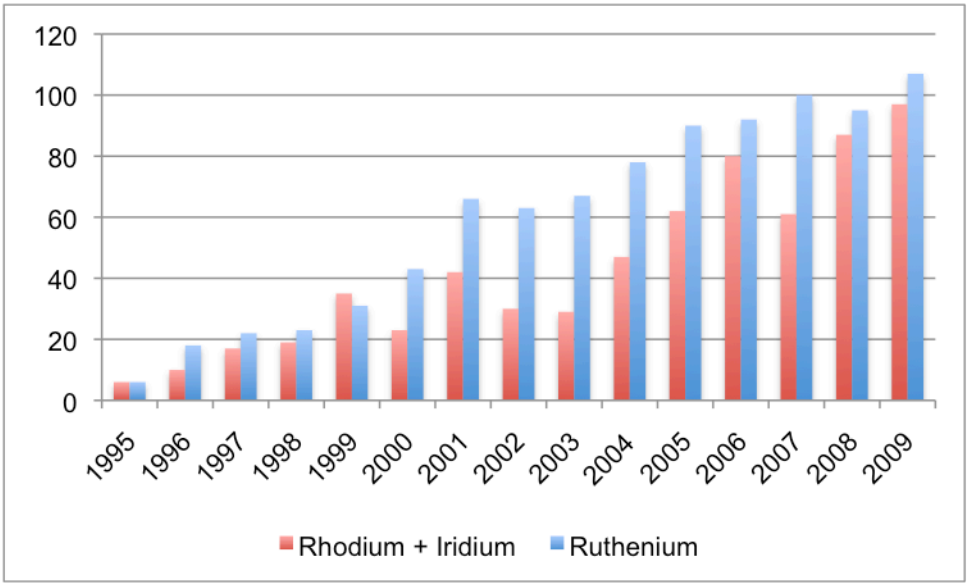

Figure 15: Number of publications containing the concept of transfer hydrogenation (refined with ruthenium or iridium and rhodium) [SciFinder].

More important and promising is the use of iron complexes. The first one were reported by Bianchini and coworkers. They reported that a dihydrogen complex of the type *cis*-[$FeH_2H\{P(CH_2CH_2PPh_2)_3\}](BPh_4)_2$ is capable of reducing saturated aromatic and aliphatic carbonyls with a good chemoselectivity [79].

Later on Gao and Noyori developed the tetradentate P_2N_2 and $P_2(NH)_2$ ligand systems (Figure 8) and successfully used them in combination with ruthenium, rhodium, and iridium [44-49,80]. The first tryouts to use these ligand systems in combination with iron were taken out in 2004, when Gao mixed the P_2N_2 ligands with various iron clusters *in-situ* and performed transfer hydrogenation. In the case of the reduction of 1,1-diphenylacetone using $(Et_3NH)[HFe_3(CO)_{11}]$ as metal precursor they got high *ee*'s up to 98% at a TOF of $13h^{-1}$ at 82ºC in neat *iso*-propanol. The further claim that the iron cluster stays intact during the reaction [4].

Morris furthermore used the same ligand concept to synthesize well-defined iron complexes of the type *trans*-$[Fe(NCCH_3)_2P_2N_2]X_2$ and *trans*-$[Fe(NCCH_3)_2P_2(NH)_2]X_2$ [3,6,7,61], he even enhanced the complex synthesis to a template synthesis, which makes it easy to access a large palette of different complexes in a one pot reaction [5]. This complexes are stable to air for several hours and soluble in DCM, $CHCl_3$, acetonitrile, and DMSO, but not in Et_2O, THF, various hydrocarbons and *iso*-propanol. After the addition of an alkoxide base the solubility changes, yielding in a highly reactive transfer hydrogenation catalyst [7]. The activities at room temperatures are as good as, or even better as those from ruthenium and rhodium complexes, which are commonly used for transfer hydrogenation [6].

12.6 Results and Discussion

The remarkable results shown by Morris and coworkers inspired our group to use the Fe(II) PNP-pincer type complexes in the field of transfer hydrogenation. The reactions were carried out in neat *iso*-propanol with 1% catalyst and 5% base loading at a temperature of 80ºC. The substrate for the screenings was acetophenone with a concentration of 0.2 $mol \cdot L^{-1}$. In general, all complexes underwent a color change after addition of base, which means that they react with the base thereby forming an active complex. This intermediate immediately decomposes on exposure to air. Their catalytic activity towards hydrogen transfer from *iso*-propanol to acetophenone is shown in Table 6.

Table 6: Results of transfer hydrogenation of *iso*-propanol to acetophenone.

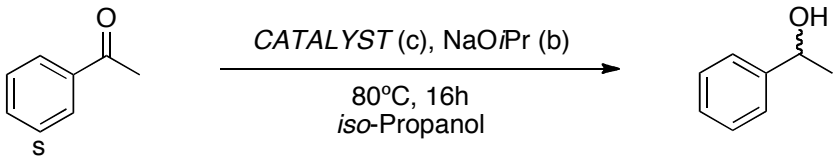

c(s) = 0.2 mol*L^{-1}
c:b:s = 1:5:100

No	Complex (c)	Base (b)	Ratio (c:b:s)	Yield [%]
1	[Fe(PNP-*i*Pr)Cl_2] (**5**)	NaO*i*Pr	1:1:100	0.7
2	*trans*-[Fe(PNP-*i*Pr)(CO)Cl_2] (**6**)	NaO*i*Pr	1:1:100	0.0
3	*trans*-[Fe(PNP-*i*Pr)$(CO)_2$Cl]BF_4 (**7**)	NaO*i*Pr	1:1:100	0.0
4	[Fe(PNP-*i*Pr)AN_3]$(BF_4)_2$ (**8**)	NaO*i*Pr	1:1:100	0.0
5	[Fe(PNP-Ph)AN_3]$(BF_4)_2$ (**9**)	NaO*i*Pr	1:1:100	0.0
6	[Fe(PNP-Ph)AN(NN-Eth,Cy)]$(BF_4)_2$ (**11**)	NaO*i*Pr	1:1:100	0.0
7	Blank	NaO*i*Pr	0:5:100	0.8
8	[Fe(PNP-Ph)AN(NN-Eth,Cy)]$(BF_4)_2$ (**11**)	NaO*i*Pr	1:5:100	1.0
9	Blank	NaO*i*Pr	0:10:100	37.0
10	[Fe(PNP-Ph)AN(NN-Eth,Cy)]$(BF_4)_2$ (**11**)	NaO*i*Pr	1:10:100	14.2
11	[Fe(PNP-*i*Pr)Cl_2] (**5**)	NaO*i*Pr	1:5:100	11.0
12	*trans*-[Fe(PNP-*i*Pr)(CO)Cl_2] (**6**)	NaO*i*Pr	1:5:100	11.7
13	*trans*-[Fe(PNP-*i*Pr)$(CO)_2$Cl]BF_4 (**7**)	NaO*i*Pr	1:5:100	15.3
14	[Fe(PNP-*i*Pr)AN_3]$(BF_4)_2$ (**8**)	NaO*i*Pr	1:5:100	0.8
15	[Fe(PNP-Ph)AN_3]$(BF_4)_2$ (**9**)	NaO*i*Pr	1:5:100	0.0

In entries 1-5, and 8 one percent base was used. It is evident that the base concentration is too low to sufficiently activate the complex since no conversion was found. Therefore the base loading was raised to 5%

Entries 6-10 compare the conversion of the blank tests to those were a catalyst was present. However, even the sample with 5% base loading (entry 7) gave a very poor conversion of 0.8%. For the blank test with 10% base loading (entry 9) a conversion of 37% was observed and it is foreseeable how the influence of the MVP-type reduction is increasing. In comparison of entry 9 to entry 10 it is evident, that the complex reacts with the base yielding in a lower base concentration, which is active for the MVP-type reduction. Analogue to the results

of the hydrogenation the diimine ligand is too bulky, which makes it impossible for the substrate and the donor molecule to interact with the active side of the complex.

Entries 11-13 show the conversion of three related species. Since the complexes in entry 11 and 12 show similar low reactions it is plausible that they might follow the same reaction mechanism. In analogy to the discoveries in the field of hydrogenation it is apparent that the *iso*-propoxide base replaces at least one chloride coordinated at the iron center with a further β-elimination probably yielding an iron hydride species, which we could as yet not been determined.

Entries 14 and 15 show that complexes **8** and **9** are catalytically inactive. All in all it is evident that Fe(II) PNP-pincer complexes are not able to perform efficient hydrogen transfer from *iso*-propanol to acetophenone. It is also impossible to raise the base concentration due to side reactions. The only possibility to use this type of complexes is in kinetic resolution of racemic mixtures, which are produced *in-situ* by MVP reduction. The drawback of this kind of complexes is the low reactivity, which is too low to compete with commercially used transfer hydrogenation complexes.

A further point of interest would be to check these complexes for their reactivity in combination with an aceotropic mixture of formic acid with triethylamine. Pincer complexes in general are very stable, so they could be stable towards the acidity of the formic acid. If this approach were successful it would be interesting to try to introduce chirality to the complex with a further screening for enantioselecivity. This work still needs to be done in future investigations.

13 Experimental

13.1 Ligands

13.1.1 PNP-Ligands

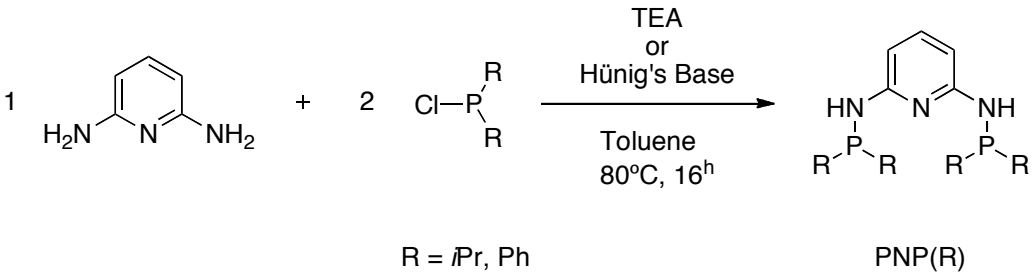

Scheme 18: General reaction scheme for the synthesis of PNP-R.

2,6-Diaminopyridine (DAP) was re-crystallized from $CHCl_3$ yielding a snow white to slightly yellow solid. All further procedures were carried out under inert gas atmosphere using schlenk techniques.

1 equiv. DAP was suspended in toluene and Hünig's base (triethylamine is also possible) was added. The mixture was cooled to 0°C and 2 equiv. of the phosphinochloride were slowly added. The reaction mixture was heated to 80°C for about 16h.

The formed amine-HCl salt was filtered off, leaving back a yellow solution. After the evaporation of toluene until a white wax like solid (if not, the yellowish honey like liquid should be put in the freezer, in order to get solid) formed.

***N,N'*-Bis(diisopropylphosphino)-2,6-diaminopyridine (PNP-*i*Pr)**

^{1}H NMR ($CDCl_3$, 20°C) δ [ppm]: 7.3 (t, $J_{HH(3\text{-}4)}$ = 8.0 Hz, $J_{HH(3\text{-}5)}$=2.4, 1H, py(H^4)), 6.4 (dd, $J_{HH(3\text{-}4)}$ = 8.0 Hz, $J_{HH(3\text{-}5)}$=2.2, 2H, py($H^{3,5}$)), 4.4 (s, 1H, NH), 1.8-1.7 (m, 4H, $CH(CH_3)_2$), 1.0-1.1 (m, 24H, $CH(CH_3)_2$).

$^{13}C\{^1H\}$ NMR ($CDCl_3$, 20ºC) δ [ppm]: 159.5 (d, *J* = 20.3 Hz, $py^{2,6}$), 139.1 (py^4), 98.1 (d, *J* = 18.4 Hz, $py^{3,5}$), 26.3 (d, *J* = 10.7 Hz,$CH(CH_3)_2$), 18.6 (d, *J* = 19.6 Hz, $CH(CH_3)_2$), 17.1 (d, *J* = 7.7 Hz, $CH(CH_3)_2$).

$^{31}P\{^1H\}$ NMR ($CDCl_3$, 20ºC) δ [ppm]: 48.3.

***N,N'*-Bis(diphenylphosphino)-2,6-diaminopyridine (PNP-Ph)**

^1H NMR ($CDCl_3$, 20ºC) δ [ppm]: 7.5-7.4 (m, 8H), 7.4-7.3 (m, 13H), 6.5 (dd, $J_{HH(3-4)}$ = 7.89 Hz, $J_{HH(3-5)=1.55,}$ 2H, py($H^{3,5}$)), 5.0 (s, 2H, NH).

$^{13}C\{^1H\}$ NMR ($CDCl_3$, 20ºC) δ [ppm]: 157.6 (d, *J* = 20.2 Hz, $py^{2,6}$), 139.9 (d, *J* = 12.1 Hz, py^4), 134.0 (Ph^1), 131.3 (d, *J* = 20.9 Hz, $Ph^{2,6}$), 129.2 (Ph^4), 128.5 (d, *J* = 6.7 Hz, $Ph^{3,4}$), 99.2 (d, *J* = 14.8 Hz, $py^{3,5}$).

$^{31}P\{^1H\}$ NMR ($CDCl_3$, 20ºC) δ [ppm]: 26,48.

13.2 Iron-Precursors

Iron(II) tetrafluoroborate hexahydrate

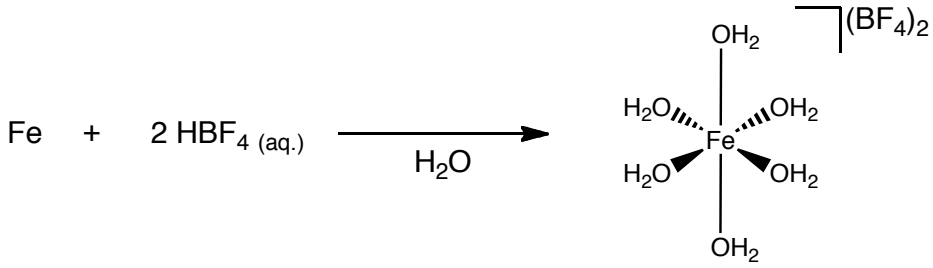

Scheme 19: General reaction scheme for the synthesis of $Fe(BF_4)_2 \cdot 6H_2O$.

Iron powder was reduced under hydrogen for 2h at 400ºC [81]. Powder-XRD measurements (Figure 16) pointed out that the iron powder was clean. Five gram of the reduced iron powder was suspended in 200 ml water, and the suspension was cooled to 0ºC; after 27 ml HBF_4 (48% aqueous-solution) were added. The reaction was stirred over night, until the iron powder was dissolved. The solution was filtered off, and the aqueous phase was reduced using a rotary evaporator, until the first crystals formed. The greenish solution was put into the freezer, to precipitate the Fe(BF4)·6 H2O. The crystals were filtered off, and washed several times with freshly distilled Et_2O (peroxide free), and tried in vacuum.

The final product is a slightly greenish solid.

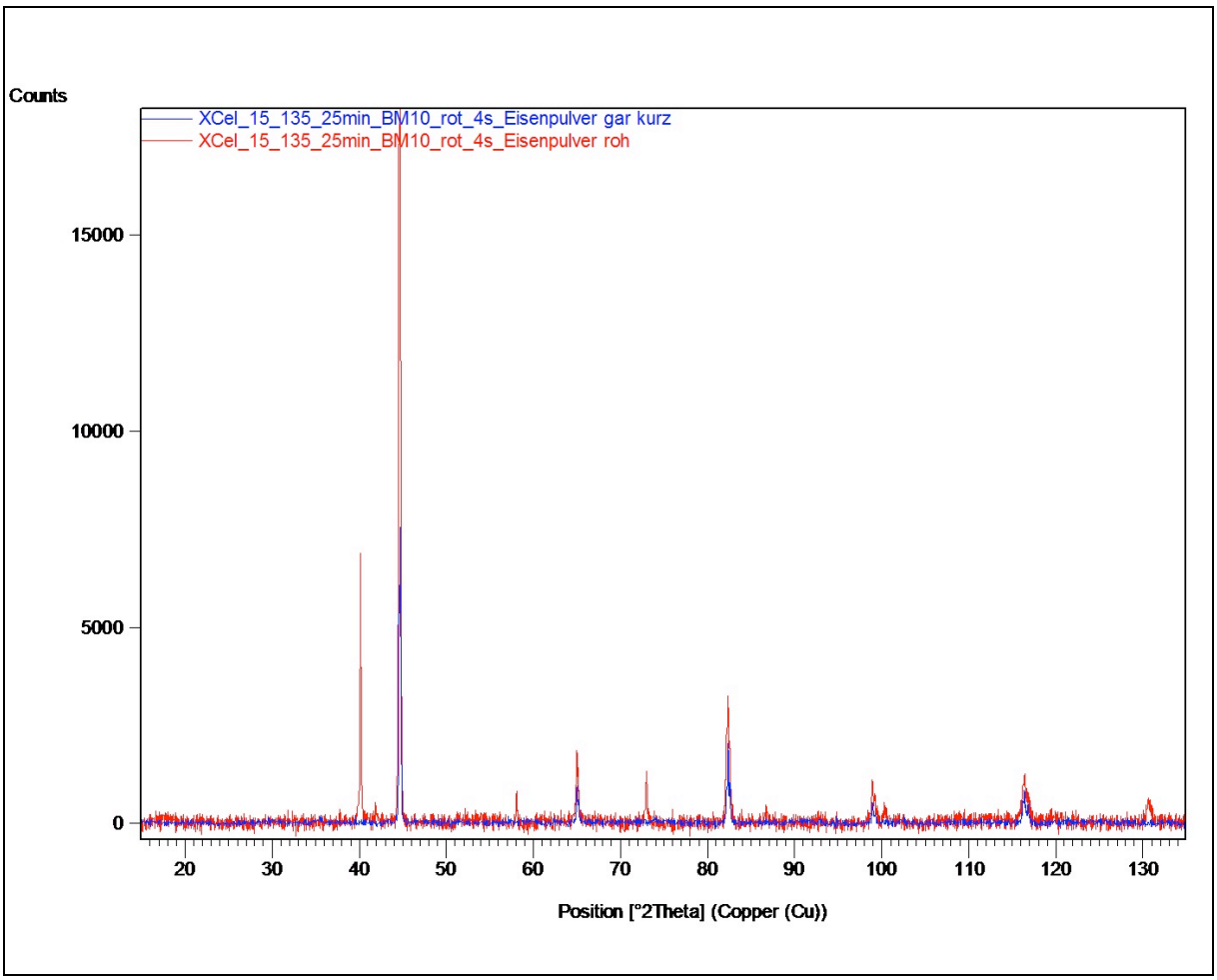

Figure 16: Powder-XRD of iron powder.

It is evident that the reflexes at an angle of 40º, 58º, 73º, and 131º, which are related by the literature to iron-oxides disappear after reduction with hydrogen. This means that only pure iron was taken to dissolve in aqueous HBF_4.

Iron(II)hexakisacetonitril tetrafluoroborate

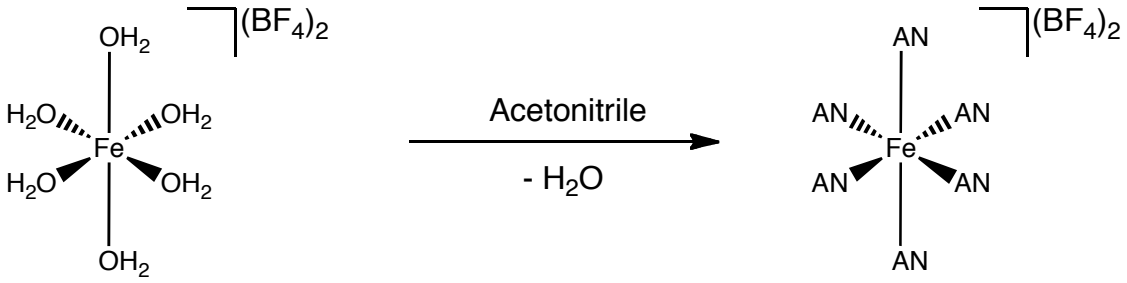

Scheme 20: Reaction scheme of $Fe(BF_4)_2 \cdot 6\ H_2O$ in acetonitrile.

$Fe(BF_4)_2 \cdot 6\ H_2O$ was dissolved in acetonitrile under argon atmosphere. The solution was refluxed in a Soxhlet-extractor filled with 3Å molecular sieve for 1 week. The solvent was evaporated under reduced pressure yielding a greenish-white fine powder.

13.3 Complexes

13.3.1 PNP-Complexes

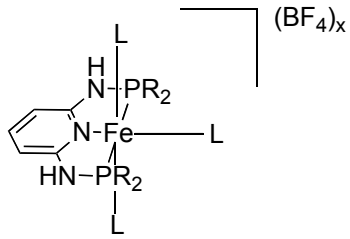

$[Fe(PNP\text{-}R)L_3](BF_4)_x$
R = *i*Pr, Ph
x = 0-2

Figure 17: General figure of the complexes using PNP(R) ligands.

If not marked different, all complexes are synthesized under inert gas atmosphere using standard schlenk techniques. The solid complexes are usually stable to air, for several hours.

1.05 equivalents of the ligand were dissolved in a schlenk tube and 1 equivalent of the iron precursor was added under vigorous stirring. The solution was stirred over night. The solvent was reduced to about 1-2 ml and freshly distilled diethyl ether (peroxide free) was added slowly to precipitate the complex. The remaining solid was washed twice with freshly distilled diethyl ether, and characterized by NMR. All solid complexes are stable to air for several hours.

[Fe(PNP-*i*Pr)Cl$_2$] (5)

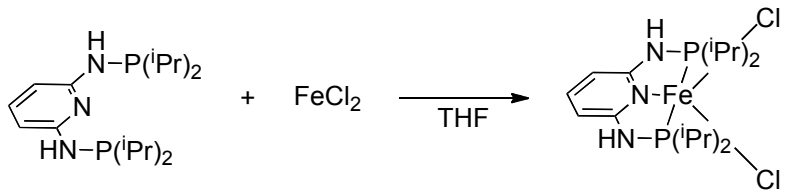

[Fe(PNP-*i*Pr)Cl$_2$]
5

Scheme 21: [Fe(PNP-*i*Pr)Cl$_2$] (5).

^{1}H NMR (d$_6$-Acetone, 20ºC, all peaks appear as broad singuletts): δ = 140,4 (CH(CH$_3$)$_2$), 75.3 (NH), 47.5 (*py*^{3,5}), 13.1 (CH(CH$_3$)$_2$), 7.0 (CH(CH$_3$)$_2$), -21.3 (*py*^{4}).

***trans*-[Fe(PNP-*i*Pr)(CO)Cl$_2$] (6)**

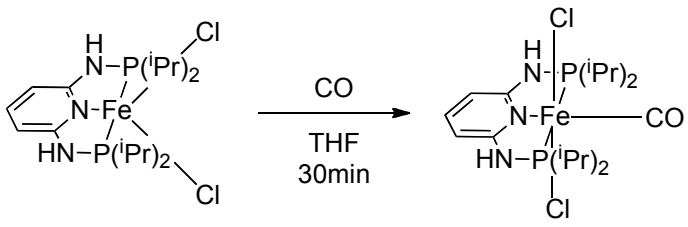

trans-[Fe(PNP-*i*Pr)(CO)Cl$_2$]
6

Scheme 22: *trans*-[Fe(PNP-*i*Pr)(CO)Cl$_2$] (6).

5 was dissolved in THF and CO was bubbled into the solution. There was an immediate color change, and a blue solid formed. The solution was stirred for additional 30 min in a CO atmosphere. The blue solid was filtered off, and washed with Et_2O twice.

^{1}H NMR (d_6-DMSO, 20ºC) δ [ppm]: 8.5 (s, 2H, NH), 7.4 (t, J=7.2Hz, 1H, *py*^{4}), 6.5 (d, J=7.2Hz, 2H, *py*^{3,5}), 2.8 (m, 4H, $CH(CH_3)_2$), 1.4 – 1.3 (m, 24H, $CH(CH_3)_2$).

^{13}C{^{1}H}-NMR (d_6-DMSO, 20ºC) δ [ppm]: 224.8 (t, *J* = 22.7 Hz, CO), 163.1 (t, *J* = 9.2 Hz, *py*^{2,6}), 139.8 (*py*^{4}), 98.7 (*py*^{3,5}), 25.5 (t, *J* = 11.8 Hz, $CH(CH_3)_2$), 19.3 ($CH(CH_3)_2$), 18.1 ($CH(CH_3)_2$).

^{31}P{^{1}H}-NMR (d_6-DMSO, 20ºC) δ [ppm]: 122.5.

IR (ATR): 1956 cm^{-1} ($\nu_{C=O}$).

UV/VIS (powder samples measured in diffuse reflectance): λ_{max} = 578 nm.

***trans*-[Fe(PNP-*i*Pr)(CO)$_2$Cl](BF$_4$) (7)**

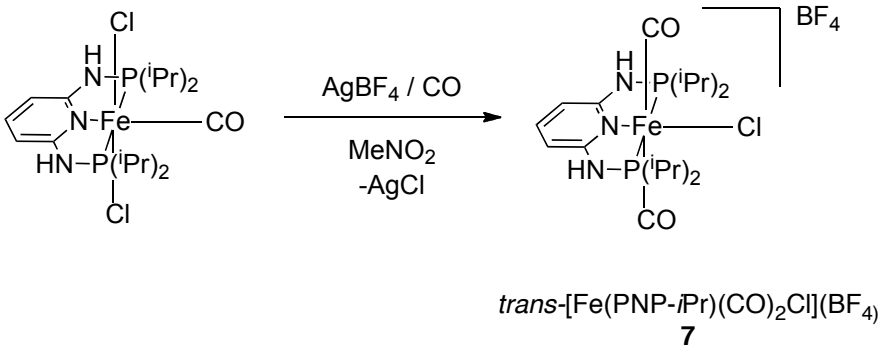

trans-[Fe(PNP-*i*Pr)(CO)$_2$Cl](BF$_4$)
7

Scheme 23: *trans*-[Fe(PNP-*i*Pr)(CO)$_2$Cl](BF$_4$) (7).

6 was dissolved in nitromethane and $AgBF_4$ was added. After CO was bubbled through the solution, which led to a color change to deep red. The solution was stirred under CO atmosphere for additional 30min. The AgCl was separated from the solution, by simply passing it through a column filled with celite. The filtrate was reduced to about 1-2 ml and precipitated by adding Et_2O. The precipitate was filtered off, and washed twice with Et_2O.

[Fe(PNP-R)(AN)$_3$](BF$_4$)$_2$ (8 & 9)

[Fe(PNP-R)(AN)$_3$](BF$_4$)$_2$
R = ^{i}Pr **8**
R = Ph **9**

Scheme 24: [Fe(PNP-R)(AN)$_3$](BF$_4$)$_2$ (8 & 9).

[Fe(PNP-iPr)(AN)$_3$](BF$_4$)$_2$ (8)

^{1}H NMR (CD$_3$CN, 20°C) δ [ppm]: 7.3 (s, 2H, NH), 7.2 (s, 1H, py^4), 6.32 (s, 2H, py^{3,5}), 3.0 (s, 4H, CH(CH$_3$)$_2$), 2.0 (s, 9H, CH$_3$CN), 1.4 (s, 12H, CH(CH$_3$)$_2$).

^{13}C{^{1}H} NMR (CDCl$_3$, 20°C) δ [ppm]: 164.1 (t, *J* = 8.1 Hz, py^{2,6}), 140.6 (py^4), 138.3 (CH$_3$CN), 99.1 (py^{3,5}), 26.8 (t, *J* = 10.1 Hz, C*H*(CH$_3$)$_2$), 17.6 (CH(C*H*$_3$)$_2$), 17.3 (CH(C*H*$_3$)$_2$), 4.4 (CH$_3$CN).

^{31}P{^{1}H} NMR (CDCl$_3$, 20°C) δ [ppm]: 115.1.

[Fe(PNP-Ph)(AN)$_3$](BF$_4$)$_2$ (9)

^{1}H NMR (CD$_3$CN, 20°C) δ [ppm]: 8.4 (s, 2H, NH), 7.9-7.6 (m, 21H, Ph, py^4), 6.6 (d, *J* = 8.0, 2H, py^{3,5}), 2.0 (s, 9H, CH$_3$CN)

^{13}C{^{1}H} NMR (CD$_3$CN, 20°C) δ [ppm]: 163.2 (t, *J* = 9.8 Hz, py^{2,6}), 141.2 (py^4), 137.7 (CH$_3$CN), 136.7 (Ph^1), 131.0 (Ph^4), 129.2 (Ph^{3,5}), 100.9 (py^{3,5}), 3.4 (CH$_3$CN).

^{31}P{^{1}H} NMR (CDCl$_3$, 20°C) δ [ppm]: 103.9.

***cis*-[Fe(PNP-Ph)(AN)$_2$CO](BF$_4$)$_2$ (10)**

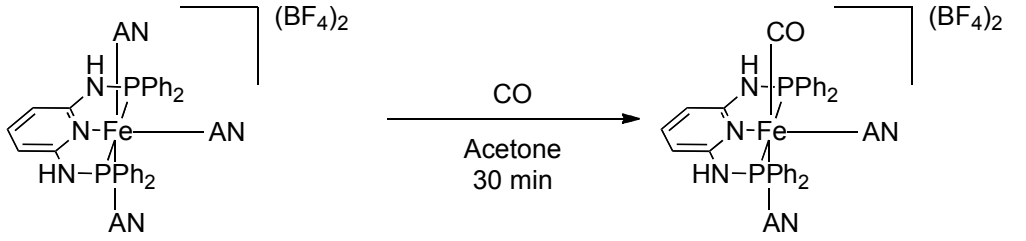

cis-[Fe(PNP-Ph)(AN)$_2$CO](BF$_4$)$_2$
10

Scheme 25: *cis*-[Fe(PNP-Ph)(AN)$_2$CO](BF$_4$)$_2$ (10).

The procedure is analogous to *trans*-[Fe(PNP-*i*Pr)(CO)Cl$_2$].

^{1}H NMR (d$_6$-Acetone, 20°C) δ [ppm]: 9.2 (s, 2H, NH), 8.0-7.8 (m, 7H, Ph, py^{4}), 7.6 – 7.4 (m, 14H, Ph), 6.7 (d, *J* = 7.4 Hz, 2H, py^{3,5}), 2.6 (s, 3H, CH$_3$CN), 1.6 (s, 3H, CH$_3$CN)

^{13}C{^{1}H} NMR (d$_6$-Acetone, 20°C) δ [ppm]: 212.4 (t, *J* = 27.0 Hz, CO), 162.6 (t, *ij = 8.3 Hz, py*^{2,6}), 143.6 (py^{4}), 140.2 (Ph^{1}), 133.4 (CH$_3$CN), 133.1 (CH$_3$CN), 132.1 – 131.7 (m, Ph), 130.7 – 130.4 (m, Ph), 103.2 (t, *J* = 4.1 Hz, py^{3,5}), 5.1 (CH$_3$CN), 3.4 (CH$_3$CN).

^{31}P{^{1}H} NMR (d$_6$-Acetone, 20°C) δ [ppm]: 95.9.

IR (KBr, cm^{-1}): 2021 ($\nu_{C=O}$)

[Fe(PNP-Ph)AN(NN-Eth,Cy)](BF$_4$)$_2$ (11)

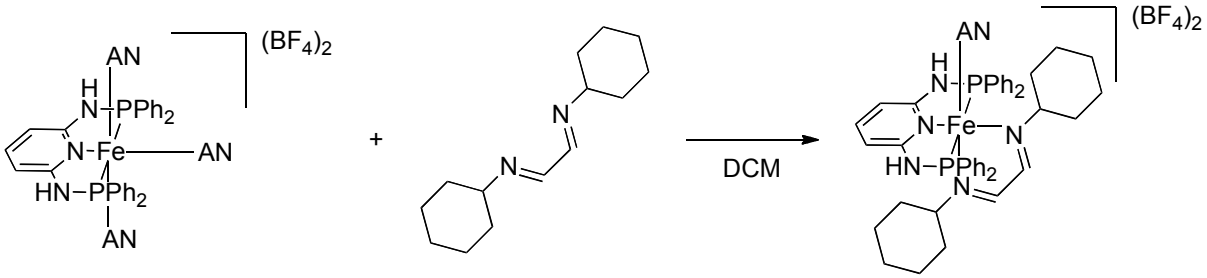

[Fe(PNP-Ph)AN
(NN-Eth,Cy)](BF4)2
11

Scheme 26: [Fe(PNP-Ph)AN(NN-Eth,Cy)](BF$_4$)$_2$ (11).

9 and the NN-Eth,Cy ligand was mixed and DCM for about 2 hours. The work up is analogous to the general proceture.

^{1}H NMR (d_6-Acetone, 20°C): Spectrum was not analyzable due to impurities.

^{31}P{^{1}H} NMR (d_6-Acetone, 20°C) δ [ppm]: 95.9.

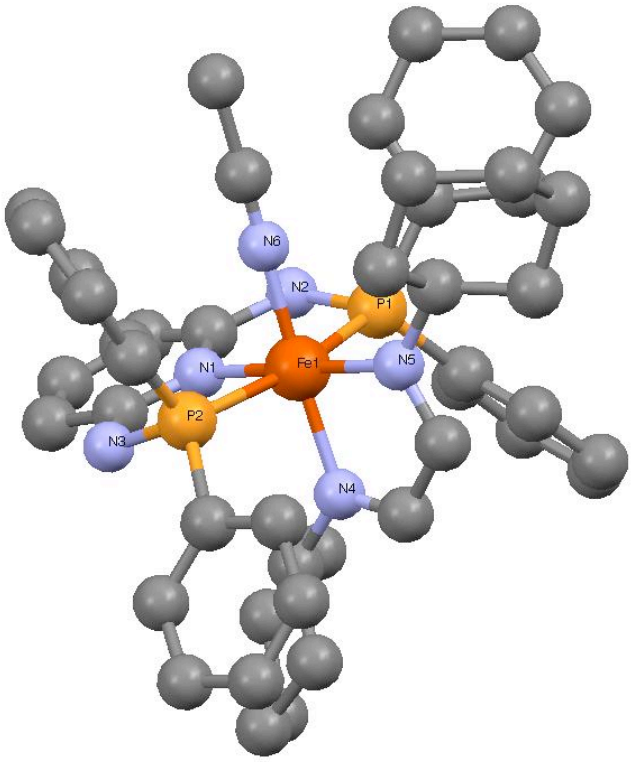

Figure 18: 3D-structure of 11 determined by XRD-messurements.

The crystals of complex 11 were crystallized from a solution of 11 in d_6-acetone by diffusion of Et_2O.

Table 7: Selected bond lengths [Å] and angles [º] of complex 11.

Bond	Length [Å]	Bonds	Angle [Å]
Fe(1)-N(5)	1.932(7)	N(5)-Fe(1)-N(6)	92.1(3)
Fe(1)-N(6)	1.936(8)	N(5)-Fe(1)-N(4)	81.4(3)
Fe(1)-N(4)	1.989(7)	N(6)-Fe(1)-N(4)	172.7(3)
Fe(1)-N(1)	1.993(7)	N(5)-Fe(1)-N(1)	176.1(3)
Fe(1)-P(1)	2.259(3)	N(6)-Fe(1)-N(1)	90.0(3)
Fe(1)-P(2)	2.266(3)	N(4)-Fe(1)-N(1)	96.6(3)
P(1)-N(2)	1.689(7)	N(5)-Fe(1)-P(1)	93.7(2)
P(2)-N(3)	1.692(7)	N(6)-Fe(1)-P(1)	86.8(2)
		N(4)-Fe(1)-P(1)	96.9(2)
		N(1)-Fe(1)-P(1)	83.2(2)
		N(5)-Fe(1)-P(2)	101.3(2)
		N(6)-Fe(1)-P(2)	89.9(2)
		N(4)-Fe(1)-P(2)	88.1(2)
		N(1)-Fe(1)-P(2)	82.0(2)
		P(1)-Fe(1)-P(2)	164.8(10)

Table 8: Crystal data, data collection parameters and refinement details for 11.

Crystal Data of $[C_{45}H_{52}FeN_6P_2]^{2+}$ $2(BF_4)^- \cdot 0.5(C_4H_{10}O)$		
M_r	1003.40	
Crystal system	monoclinic	
Space group	$P2_1/n$	
Temperature	113(2) K	
Wavelength	0.71075 Å	
Unit cell dimensions	a = 10.976(5) Å b = 20.459(9) Å c = 24.835(12) Å	α = 90° β = 98.51(4)° γ = 90°
Volume	5515(4) Å^3	
Z	4	
Density (calculated)	1.208 Mg/m^3	
Absorption coefficient	0.394 mm^{-1}	
Crystal form and color	red thin needles	
Crystal size	0.46 x 0.10 x 0.06 mm^3	
Data Collection		
T_{min}, T_{max}	0.8394, 0.9767	
Final R indices [I>2σ(I)]*	R_1 = 0.1280, ωR_2 = 0.2738	
Completeness to Θ = 27.28°	85.8 %	
Independent reflections	10629 [R_{int} = 0.1848]	
Reflections collected	36779	
Theta range for data collection	4.65 to 27.28°.	
Index ranges	-13 ≤ h ≤ 13 -26 ≤ k ≤ 26 -31 ≤ l ≤ 31	
Refinement		
Refinement method	Full-matrix least-squares on F^2	
Data / restraints / parameters	10629 / 0 / 625	
Goodness-of-fit on F^2	1.187	
R indices (all data)	R_1 = 0.2775, ωR_2 = 0.3265	
Largest diff. peak and hole	1.831 and -0.558 e.Å^{-3}	

*The R-values are high due to the presence of Et_2O in the crystal lattice.

14 List of Abbreviations

aq	aqueous
AN	Acetonitrile
BINAP	2,2´–Bis(diphenylphosphino)–1,1´–binaphthyl
$CHCl_3$	Chloroform
CH_2Cl_2	Methylenechloride
Cod	1,5-Cyclooctadien
cp	cyclopentadienyl
DAIPEN	1,1-bis(4-methoxyphenyl)-3-methylbutane-1,2-diamine
DAP	Pyridine-2,6-diamine
DCM	Dichloromethane
DFT	Density Functional Theory
DME	Dimethoxyethane
DMSO	Dimethylsulfoxide
ED	electron donating
equs.	Equivalents
Et_2O	Diethylether
EW	electron withdrawing
Hünig's base	diisopropylethylamine
i	*iso*
IR	infrared
Me	Methyl
$MeNO_2$	Nitromethane
MPV-reduction	Meerwein-Ponndorf-Verley reduction
NMDPP	neomenthyldiphenylphosphine

NMR	Nuclear Magnetic Resonance
PMMA	Polymethylmethacrylate
R.T.	room temperature
t	*tertiary*
TEA	Triethylamine
THF	Tetrahydrofuran
TMS	Trimethylsilan
TOF	Turn Over Frequency
Tol	Toluene
TON	Turn Over Number
UV/VIS	Ultraviolet / Visible
XRD	X-Ray Diffraction

15 References

(1) Enthaler, S.; Hagemann, B.; Erre, G.; Junge, K.; Beller, M. *Chemistry-an Asian Journal* **2006**, *1*, 598.

(2) Enthaler, S.; Junge, K.; Beller, M. *Angewandte Chemie-International Edition* **2008**, *47*, 3317.

(3) Meyer, N.; Lough, A. J.; Morris, R. H. *Chemistry-a European Journal* **2009**, *15*, 5605.

(4) Chen, J. S.; Chen, L. L.; Xing, Y.; Chen, G.; Shen, W. Y.; Dong, Z. R.; Li, Y. Y.; Gao, J. X. *Acta Chim. Sin.* **2004**, *62*, 1745.

(5) Mikhailine, A. A.; Kim, E.; Dingels, C.; Lough, A. J.; Morris, R. H. *Inorganic Chemistry* **2008**, *47*, 6587.

(6) Morris, R. H. *Chemical Society Reviews* **2009**, *38*, 2282.

(7) Sui-Seng, C.; Freutel, F.; Lough, A. J.; Morris, R. H. *Angewandte Chemie-International Edition* **2008**, *47*, 940.

(8) Trovitch, R. J.; Lobkovsky, E.; Chirik, P. J. *Inorganic Chemistry* **2006**, *45*, 7252.

(9) Augustine, R. L. *Marcel Dekker, INC.* **1965**.

(10) Allen, C. F. H.; Van Allen, J. *Org Synth* **1941**, *21*, 108.

(11) Mague, J. T.; Wilkinson, G. *J Chem Soc A* **1966**, 1736.

(12) Osborn, J. A.; Jardine, F. H.; Young, J. F.; Wilkinson, G. *J Chem Soc A* **1966**, 1711.

(13) Vaska, L.; Rhodes, R. E. *Journal of the American Chemical Society* **1965**, *87*, 4970.

(14) Knowles, W. S. *Angewandte Chemie-International Edition* **2002**, *41*, 1999.

(15) Izumi, Y.; Imaida, M.; Fukawa, H.; Akabori, S. *B Chem Soc Jpn* **1963**, *36*, 21.

(16) Akabori, S.; Sakurai, S.; Izumi, Y.; Fujii, Y. *Nature* **1956**, *178*, 323.

(17) Izumi, Y.; Tatsumi, S.; Imaida, M.; Fukuda, Y.; Akabori, S. *B Chem Soc Jpn* **1965**, *38*, 1206.

(18) Tatsumi, S.; Imaida, M.; Fukuda, Y.; Izumi, Y.; Akabori, S. *B Chem Soc Jpn* **1964**, *37*, 846.

(19) Korpiun, O.; Mislow, K. *Journal of the American Chemical Society* **1967**, *89*, 4784.

(20) Horner, L.; Hoffmann, H.; Beck, P. *Chem Ber-Recl* **1958**, *91*, 1583.

(21) Knowles, W. S.; Sabacky, M. J. *Chem Commun* **1968**, 1445.

(22) Morrison, J. D.; Burnett, R. E.; Aguiar, A. M.; Morrow, C. J.; Phillips, C. *Journal of the American Chemical Society* **1971**, *93*, 1301.

(23) Enthaler, S. **2007**.

(24) Blaser, H. U.; Studer, M. *Chirality* **1999**, *11*, 459.

(25) Benito-Garagorri, D.; Kirchner, K. *Accounts of Chemical Research* **2008**, *41*, 201.

(26) Moulton, C. J.; Shaw, B. L. *J Chem Soc Dalton* **1976**, 1020.

(27) Gandelman, M.; Vigalok, A.; Shimon, L. J. W.; Milstein, D. *Organometallics* **1997**, *16*, 3981.

(28) Tolman, C. A. *Journal of the American Chemical Society* **1970**, *92*, 2953.

(29) Albrecht, M.; van Koten, G. *Angewandte Chemie International Edition* **2001**, *40*, 3750.

(30) Albrecht, M.; Gossage, R. A.; Lutz, M.; Spek, A. L.; van Koten, G. *Chemistry-a European Journal* **2000**, *6*, 1431.

(31) Steenwinkel, P.; Grove, D. M.; Veldman, N.; Spek, A. L.; van Koten, G. *Organometallics* **1998**, *17*, 5647.

(32) van der Boom, M. E.; Milstein, D. *Chemical Reviews* **2003**, *103*, 1759.

(33) Hedberg, C. *Carbonyl Hydrogenation*; Wiley-VCH Verlag GmbH & Co. KGaA, 2008.

(34) Ohkuma, T.; Ooka, H.; Hashiguchi, S.; Ikariya, T.; Noyori, R. *Journal of the American Chemical Society* **1995**, *117*, 2675.

(35) Enthaler, S.; Junge, K.; Beller, M. *Reduction of Unsaturated Compounds with Homogeneous Iron Catalysts*; Wiley-VCH Verlag GmbH & Co. KGaA, 2008.

(36) Bolm, C.; Legros, J.; Le Paih, J.; Zani, L. *Chemical Reviews* **2004**, *104*, 6217.

(37) Plietker, B. *Front Matter*; Wiley-VCH Verlag GmbH & Co. KGaA, 2008.

(38) Shvo, Y.; Czarkie, D.; Rahamim, Y.; Chodosh, D. F. *Journal of the American Chemical Society* **1986**, *108*, 7400.

(39) Knölker, H. J.; Baum, E.; Goesmann, H.; Klauss, R. *Angewandte Chemie International Edition* **1999**, *38*, 2064.

(40) Casey, C. P.; Guan, H. R. *Journal of the American Chemical Society* **2007**, *129*, 5816.

(41) Casey, C. P.; Guan, H. *Journal of the American Chemical Society* **2009**, *131*, 2499.

(42) Zhang, H. H.; Chen, D. Z.; Zhang, Y. H.; Zhang, G. Q.; Liu, J. B. *Dalton Transactions* **2010**, *39*, 1972.

(43) Li, T.; Churlaud, R. l.; Lough, A. J.; Abdur-Rashid, K.; Morris, R. H. *Organometallics* **2004**, *23*, 6239.

(44) Dong, Z.-R.; Li, Y.-Y.; Chen, J.-S.; Li, B.-Z.; Xing, Y.; Gao, J.-X. *Organic Letters* **2005**, *7*, 1043.

(45) Gao, J.-X.; Ikariya, T.; Noyori, R. *Organometallics* **1996**, *15*, 1087.

(46) Gao, J.-X.; Yi, X.-D.; Xu, P.-P.; Tang, C.-L.; Wan, H.-L.; Ikariya, T. *J Organomet Chem* **1999**, *592*, 290.

(47) Gao, J. X.; Zhang, H.; Yi, X. D.; Xu, P. P.; Tang, C. L.; Wan, H. L.; Tsai, K. R.; Ikariya, T. *Chirality* **2000**, *12*, 383.

(48) Xing, Y.; Chen, J.-S.; Dong, Z.-R.; Li, Y.-Y.; Gao, J.-X. *Tetrahedron Lett* **2006**, *47*, 4501.

(49) Zhang, H.; Yang, C.-B.; Li, Y.-Y.; Donga, Z.-R.; Gao, J.-X.; Nakamura, H.; Murata, K.; Ikariya, T. *Chem Commun* **2003**, 142.

(50) Abdur-Rashid, K.; Faatz, M.; Lough, A. J.; Morris, R. H. *Journal of the American Chemical Society* **2001**, *123*, 7473.

(51) Clapham, S. E.; Hadzovic, A.; Morris, R. H. *Coordination Chemistry Reviews* **2004**, *248*, 2201.

(52) Noyori, R.; Ohkuma, T. *Angewandte Chemie-International Edition* **2001**, *40*, 40.

(53) Morris, R. H. *Can. J. Chem.-Rev. Can. Chim.* **1996**, *74*, 1907.

(54) Benito-Garagorri, D.; Alves, L. G. a.; Puchberger, M.; Mereiter, K.; Veiros, L. F.; Calhorda, M. J.; Carvalho, M. D.; Ferreira, L. P.; Godinho, M.; Kirchner, K. *Organometallics* **2009**, *28*, 6902.

(55) Benito-Garagorri, D.; Becker, E.; Wiedermann, J.; Lackner, W.; Pollak, M.; Mereiter, K.; Kisala, J.; Kirchner, K. *Organometallics* **2006**, *25*, 1900.

(56) Benito-Garagorri, D.; Bocokiƒá, V.; Mereiter, K.; Kirchner, K. *Organometallics* **2006**, *25*, 3817.

(57) Benito-Garagorri, D.; Wiedermann, J.; Pollak, M.; Mereiter, K.; Kirchner, K. *Organometallics* **2006**, *26*, 217.

(58) Takagi, H.; Isoda, T.; Kusakabe, K.; Morooka, S. *Energy & Fuels* **1999**, *13*, 1191.

(59) Walling, C.; Bollyky, L. *Journal of the American Chemical Society* **1964**, *86*, 3750.

(60) Berkessel, A.; Schubert, T. J. S.; Muller, T. N. *Journal of the American Chemical Society* **2002**, *124*, 8693.

(61) Sui-Seng, C.; Haque, F. N.; Hadzovic, A.; PuÃàtz, A.-M.; Reuss, V.; Meyer, N.; Lough, A. J.; Zimmer-De Iuliis, M.; Morris, R. H. *Inorganic Chemistry* **2008**, *48*, 735.

(62) Benito-Garagorri, D.; Puchberger, M.; Mereiter, K.; Kirchner, K. *Angewandte Chemie International Edition* **2008**, *47*, 9142.

(63) Gladiali, S.; Taras, R. *Reduction of Carbonyl Compounds by Hydrogen Transfer*; Wiley-VCH Verlag GmbH & Co. KGaA, 2008.

(64) Knoevenagel, E.; Bergdolt, B. *Ber Dtsch Chem Ges* **1903**, *36*, 2857.

(65) Wieland, H. *Ber Dtsch Chem Ges* **1912**, *45*, 484.

(66) Meerwein, H.; Schmidt, R. *Liebigs Ann Chem* **1925**, *444*, 221.

(67) Verley, A. *Bulletin de la Societe Chimique de France* **1925**, *37*, 537.

(68) Ponndorf, W. *Angewandte Chemie* **1926**, *39*, 138.

(69) Li, J. J.; Corey, E. J. *Reduction*; John Wiley & Sons, Inc., 2007.

(70) Oppenauer, R. V. *Recl Trav Chim Pay-B* **1937**, *56*, 137.

(71) Bailar, J. C.; Itatani, H. *Journal of the American Chemical Society* **1967**, *89*, 1592.

(72) Trocha-Grimshaw, J.; Henbest, H. B. *Chemical Communications (London)* **1967**, 544.

(73) Sasson, Y.; Blum, J. *Tetrahedron Lett* **1971**, 2167.

(74) Sasson, Y.; Blum, J. *Journal of Organic Chemistry* **1975**, *40*, 1887.

(75) Zassinovich, G.; Mestroni, G.; Gladiali, S. *Chemical Reviews* **1992**, *92*, 1051.

(76) Noyori, R.; Hashiguchi, S. *Accounts of Chemical Research* **1997**, *30*, 97.

(77) Zassinovich, G.; Bettella, R.; Mestroni, G.; Bresciani-Pahor, N.; Geremia, S.; Randaccio, L. *J Organomet Chem* **1989**, *370*, 187.

(78) Handgraaf, J.-W.; Reek, J. N. H.; Meijer, E. J. *Organometallics* **2003**, *22*, 3150.

(79) Bianchini, C.; Farnetti, E.; Graziani, M.; Peruzzini, M.; Polo, A. *Organometallics* **1993**, *12*, 3753.

(80) Fukui, S.; Suzuki, N.; Wada, T.; Tanaka, K.; Nagao, H. *Organometallics* **2010**, *29*, 1534.

(81) Nakamura, Y. *Proceedings of the Japan Academy* **1964**, *40*, 206.